The CLAS12 Geant4 Simulation

M. Ungaro[a,*], G. Angelini[l], M. Battaglieri[b], M. Contalbrigo[n], V. D. Burkert[a], D. S. Carman[a], P. Chatagnon[e],
M. Defurne[c], B. Duran[k], R. De Vita[b], R. Fair[a], M. Garçon[c], Y. Gotra[a], P. Ghoshal[a], R. Rajput-Ghoshal[a], S. Joosten[o],
A. Kim[d], D. Lersch[j], N. Markov[d], M.D. Mestayer[a], R. Miller[a], M. Mirazita[m], J. Newton[h], S. Niccolai[e], W. Phelps[l],
S. Procureur[c], Y. Prok[h,1], A. Puckett[d], D. Sokhan[f], S. Stepanyan[a], A. Vlassov[g], R, Wang[e], C. Wiggins[a], V. Ziegler[a]

[a]*Thomas Jefferson National Accelerator Facility, Newport News, VA 23606, USA*
[b]*Istituto Nazionale Di Fisica Nucleare, 16146 Genova, Italy*
[c]*IRFU, CEA, Université Paris-Saclay, F-91191 Gif-sur-Yvette, France*
[d]*University of Connecticut, Storrs, Connecticut 06269, USA*
[e]*Institut de Physique Nuclaire, CNRS-IN2P3, Univ. Paris-Sud, Universit Paris-Saclay, 91406 Orsay Cedex, France*
[f]*University of Glasgow, Glasgow G12 8QQ, United Kingdom*
[g]*Institute For Theoretical and Experimental Physics, Ulitsa, 25 Moscow, Russia, 117218*
[h]*Old Dominion University, Norfolk, VA 23529, USA*
[i]*Virginia Commonwealth University, Richmond, VA 23284, USA*
[j]*Florida State University, Tallahassee, FL 32306, USA*
[k]*Temple University, Philadelphia, PA 19122, USA*
[l]*George Washington University, Washington, DC 20052, USA*
[m]*Istituto Nazionale Di Fisica Nucleare, 00044 Frascati (Roma), Italy*
[n]*Istituto Nazionale Di Fisica Nucleare, 44122 Ferrara, Italy*
[o]*Argonne National Laboratory, Lemont, IL 60439, USA*

Abstract

The Geant4 Monte-Carlo (GEMC) package is used to simulate the passage of particles through the various CLAS12 detectors. The geometry is implemented through a database of Geant4 volumes created either through the GEMC native API, by the CLAS12 geometry service, or imported from the CAD engineering model. The truth information is digitized with a plugin mechanism by routines specific to each detector and includes the use of the CLAS12 calibration database constants to produce both ADC and TDC response functions. Theoretical models that produce the generated events interface with GEMC through the LUND data format. The merging of simulated data with real random trigger data provides a mechanism to include both beam and electronic background into the simulation of generated events to accurately model beam data from the CLAS12 detector. The performance of simulation is demonstrated by comparison with the experimental data.

Keywords: Geant4, GEMC, simulation, software, database, Monte Carlo, cad, stl, gdml, mysql, C++.

1. Overview

The CEBAF Large Acceptance Spectrometer for operation at 12 GeV beam energy (CLAS12) [1] in Hall B at the Thomas Jefferson National Accelerator Facility (Jefferson Lab) was designed to study electro-induced nuclear and hadronic reactions by providing efficient detection of charged and neutral particles over a large fraction of the full solid angle. CLAS12 is based on two superconducting magnets and multiple detector subsystems that provide large coverage for the detection of charged and neutral particles produced by the interaction of the electron beam from the JLab CEBAF accelerator with a target located at the center of the spectrometer. A six-coil torus magnet [2] defines the six-sector structure of the so-called Forward Detector that is outfitted with Drift Chambers [3] for charged particle tracking and multiple detector systems for particle identification. These detectors include threshold Cherenkov Counters [4, 5] and Ring-Imaging Cherenkov Counters [6], scintillator-based time-of-flight hodoscopes [7], and electromagnetic calorimeters [8]. In the target region, a 5 T superconducting solenoid [2] surrounds a central tracker based on silicon and Micromegas detectors [9, 10], and subsystems for particle identification

---

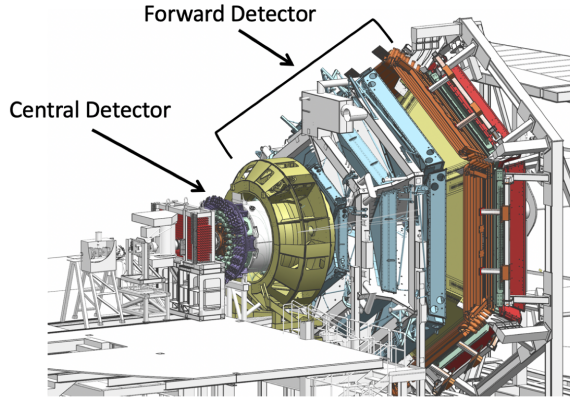*Corresponding author
Email address:* ungaro@jlab.org (M. Ungaro)

Figure 1: Model representation of the CLAS12 spectrometer in Hall B at Jefferson Laboratory. The electron beam is incident from the left side of this figure. The CLAS12 detector is roughly 20 m in scale along the beam axis. The CLAS12 Forward and Central Detectors are identified.
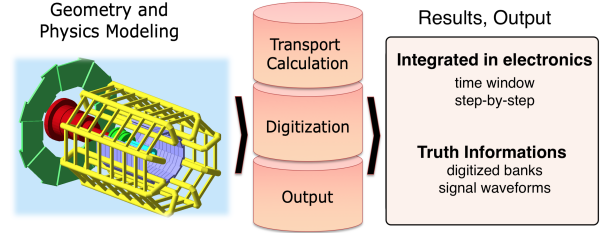

Figure 2: The architecture of GEMC. The simulation parameters are stored in an external database. GEMC collects them and organizes the necessary Geant4 ingredients used to simulate the passage of particles through materials and sensitive regions. The hits are digitized with plugins defined by the user and collected in user-defined outputs.

that include a time-of-flight scintillation counter barrel [11] and a neutron detector [12], forming the so-called Central Detector.

A model representation of the CLAS12 spectrometer identifying the Forward and Central Detectors is shown in Fig. 1. In between the central and forward regions, the CLAS12 Forward Tagger [13] extends the kinematic coverage for the detection of electrons and photons at polar angles from $2°$ to $5°$. The total number of readout channels of CLAS12 is larger than 100k. Typical trigger rates are 15 kHz. In 2018, data rates of 500 MB/s with a live time of >95% were achieved.

The spectrometer has met the performance criteria of instantaneous luminosity up to 10^{35} cm^{-2}s^{-1} and momentum resolution σ_p/p in the forward direction using the drift chambers and in the central direction using the vertex tracker of < 1% and < 3%, respectively.

The CLAS Collaboration has implemented a detector simulation within the GEMC software framework [14]. During the design phase of the various CLAS12 detectors, shielding, magnets, and passive elements, GEMC allowed for studies of the performance of the various components with respect to the desired science objectives. GEMC enabled the optimization of the design from trade-off studies between variation of the hardware setup and placement, and various materials and shielding thicknesses. In addition, it was instrumental in determining the rates, photomultiplier tube (PMT) currents, and radiation doses to ensure that the various detectors would survive operations during the expected spectrometer lifetime. Before and during the experiment data taking, GEMC was instrumental in preparing and understanding the calibration and measurements of the CLAS12 detectors. Finally, GEMC is used to accurately calculate the CLAS12 acceptance, including the detector response, geometrical acceptance, and tracking efficiency needed for the physics results and science goals.

GEMC is a C++ framework that uses Geant4 [15] to simulate the passage of particles through matter. It provides:

- an application-independent geometry description;

- an easy interface to build/run experiments;

- CAD/GDML imports.

The simulation parameters are stored in external databases and are used to define the Geant4 objects at run time. This includes:

- geometry;

- materials;

- mirrors;

- physics list;

- database constants;

- digitization to match the data numerical format;

- electromagnetic fields.

Particles are transported through the detector materials and produce radiation, hits, and secondaries. GEMC then collects the Geant4 results and produces the output specified by the user. The design of the framework is summarized in Fig. 2.

The following CLAS12 systems are implemented in the simulations:

2

- Various CLAS12 targets, including liquid-hydrogen, liquid-deuterium, and various solid targets;

- Silicon Vertex Tracker (SVT) [9];

- Micromegas Tracker (MM) [10];

- Central Time-of-Flight System (CTOF) [11];

- Central Neutron Detector (CND) [12];

- High Threshold Cherenkov Counter (HTCC) [5];

- Forward Tagger (FT) [13];

- Drift Chamber System (DC) [3];

- Low Threshold Cherenkov Counter (LTCC) [4];

- Forward Time-of-Flight System (FTOF) [7];

- Electromagnetic Shower Calorimeter (EC) [16];

- Pre-Shower Calorimeter (PCAL) [8];

- Ring Imaging Cherenkov Detector (RICH) [6];

- Beamline [17];

- Superconducting Magnets [2].

The CLAS12 mechanical design include electronics, support structures, and additional hardware that cannot entirely be imported in the simulation due to memory and CPU limitations: each object increases the overall system complexity, the time, and the memory needed to process events. Nevertheless, all of the elements within the particle trajectory paths to any of the CLAS12 detectors are included in the simulation. In addition, the simulation incorporates selected hardware in order to reproduce beam-related rates in the detectors to a good level of accuracy, with priority given to volumes near high background areas and near sensitive detectors.

By omitting some materials, we limit the ability of the simulation to make predictions. However, built in the simulation is the ability to merge hits using random trigger events from experimental data, which include the real background rates, as detailed in Section 1.11.

The simulation implementation is detailed in the sections below.

1.1. Geometry and Materials Import

The geometry and system materials are stored in external databases that can be MYSQL tables or text files that mimic the MYSQL tables. The databases can be defined using the following factories:

- GEMC native API (Perl or Python);

- JAVA algorithms used by both simulation and the CLAS12 event reconstruction software [18] or "JAVA geometry services";

- CAD (STL, PLY formats);

- GDML, C++ plugins (not used in CLAS12).

The GEMC native API and the CLAS12 geometry code source repositories are listed on the CLAS12 tags portal [19].

1.1.1. Importing CAD Volumes from the Engineering Model

The Hall B detectors and their supports are designed with 3D CAD software. This includes a reference system and the hierarchy of all detector elements, down to details such as nuts and bolts. The CAD models are exported into STEP files [20] (see Fig. 3). In order to import them into the GEMC simulation, the elements in the STEP file are "tessellated", a process in which polygonal triangular faucets are created to define a Geant4 volume that best represents the original CAD element. The software used to do this is FreeCad [21]. An example of tessellation showing the polygonal shapes is shown in Fig. 4. The number of faucets depends on the object complexity, and varies between 100 and 10,000. Not all of the objects are imported from the engineering model due to the following limitations:

1. memory and CPU limitations discussed above: only volumes near high-background areas and near sensitive detectors are considered;

2. when volumes that contains very small and pointy features are tessellated, the facets may be too small to be processed properly in Geant4 and cause tracks to get stuck or produce swimming errors.

The simulated CAD import is as close to reality as the engineering model is close to reality. We did encounter differences between the STEP files, the drawings, and reality in a few occasions and designed a workflow to eliminate any discrepancies. An example of comparing volumes in the GEMC simulation to the engineering drawings as part of the validation process is shown in Fig. 5.
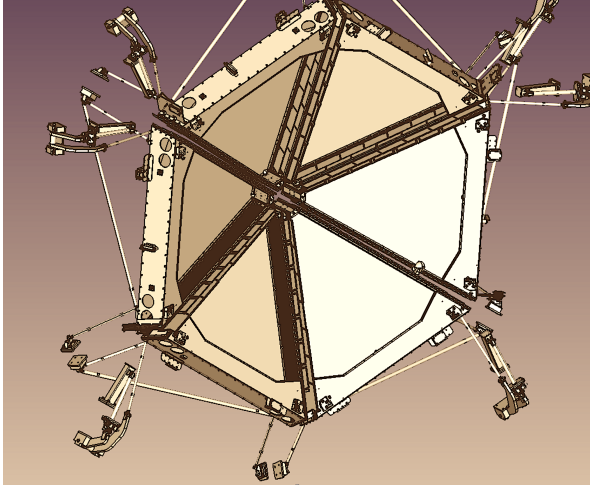
3

Figure 3: The engineering model of the CLAS12 drift chambers. Some hardware shown in this figure, for example the support structure outside the detector fiducial volume, is not imported in the simulation as explained in Section 1.

1.2. Magnetic Fields

The magnetic fields are loaded from ASCII files. The following Geant4 parameters are loaded from command line options or configuration files at run time:

- minStep: minimum track distance in the magnetic field (step) before re-computing its value;

- integralAlgorithm: compute the field value from the closest cell or using a linear (or bi-linear) interpolation;

- interpolationMethod: interpolation algorithm used to transport tracks in magnetic fields, typically a variation (choice of order and/or precision) of Runge-Kutta [22] methods.

The implementation of the CLAS12 magnetic fields is described in Section 2.13.1.

1.3. Event Time Window and Hit Definition

The Geant4 sensitive volumes are associated with a GEMC identifier that contains hierarchical information such as mother volumes and volume copy number.

Each detector is associated with a time quantity to mimic the readout electronic time window. The time window and identifier define a GEMC hit from a series of Geant4 steps: all of the steps in a given identifier that are within the time window are part of the same GEMC hit. The algorithm is illustrated in Fig. 6.
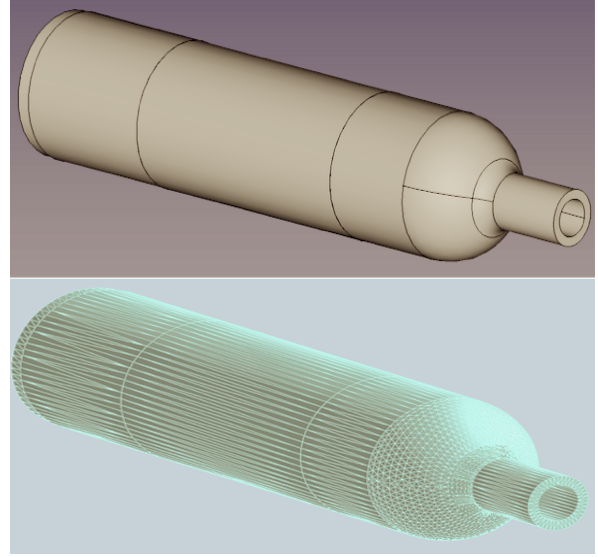

Figure 4: An example of a volume from a STEP file tessellated in GEMC. The volume that is shown is the target scattering chamber. Top: the CAD representation in the engineering model. Bottom: the tessellation.

1.4. Process Identification

A "Process ID" method can be implemented by some digitization algorithm to modify or add GEMC identifiers to each Geant4 step. For CLAS12 this happens in two cases, detailed for each detector:

- a paddle is hit but two outputs are produced because there is one PMT at each end of the scintillator. This is the case for CTOF, CND, and FTOF.

- some hardware elements are not present in the simulation. This is the case for the drift chambers, where the volumes do not contain the individual wires. In this case the wire number is calculated based on the position of the hit in the mother volume. In CLAS12 this mechanism is adopted by the DC, SVT, RICH, and MM.

1.5. CLAS12 Data Acquisition and Trigger Emulation

GEMC supports the emulation of the CLAS12 data acquisition system (DAQ) [23]. The CLAS12 data are expressed as specific collections of numbers, or "banks", that keep related numbers together. In particular, each detector channel can be associated with banks containing:

- the Flash Analog-to-Digital Converter (FADC) signal: this is the voltage signal as a function of time of the channel, sampled in 4-ns intervals;
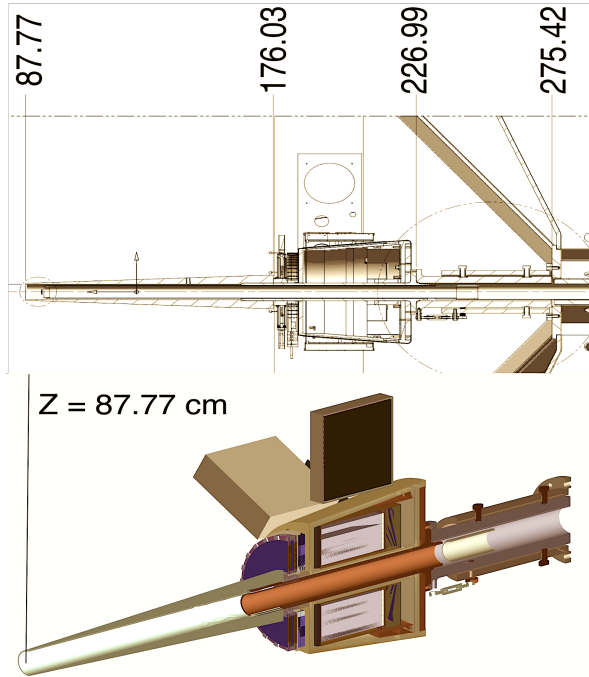
Figure 5: An example of comparing volumes in the GEMC simulation to the engineering drawings, in this case to validate the cone shield position. Top: engineering drawings of the CLAS12 beamline and shielding. The start of the Møller shielding is 87.77 cm downstream of the target center. Bottom: a geantino (a special Geant4 particle that does not interact with materials or fields) is shot vertically at z=87.77 cm, showing that the Geant4 cone position agrees with the drawings.
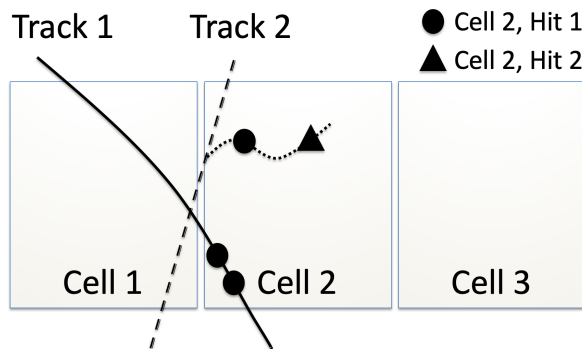

Figure 6: The GEMC hit definition algorithm. The sensitive element Cell 2 is hit by three particles, two primaries and one secondary. The Geant4 steps are drawn explicitly with circle and triangle symbols. The circle steps generated by both the primary track 1 and the secondary from track 2 are within the time window and therefore are part of the same GEMC hit "Cell 2, Hit 1". The single triangle step generated by the secondary from track 2 comes after and does not fall within the "Cell 2, Hit 1" time window; therefore it is part of a new GEMC hit, "Cell 2, Hit 2".

- the Time-to-Digital Counter (TDC) value: this represents the time of the hit in the channel relative to a common start time;

- one single value of ADC for each hit, extrapolated from the FADC voltage distribution by considering the pedestal and the channel threshold;

- one single value of TDC for each hit, extrapolated from the FADC voltage distribution by considering channel signal shape and rise time.

The FADC and TDC signals are programmed into Field Programmable Gate Arrays (FPGA) that use selection and filtering algorithms to produce a trigger for the event [24].

The simulation is able to provide both the FADC voltage signals as a function of time using the same sampling as the CLAS12 DAQ, and the ADC or TDC values extrapolated using the energy deposited or hit time. The energy deposited in each Geant4 step is convoluted with a detector-defined function that describes the electronic pulse for that energy (typically a Gaussian or Landau distribution). These signals are then summed up to provide a voltage vs. time signal, and then sampled every 4 ns to mimic the FADC. An example of a simulated vs. data FADC signal is given in Fig. 7.

The FADC simulated signal was used to program and adjust the FPGA algorithms and improve the CLAS12 trigger system, see Ref. [24].

1.6. Detectors and Hit Process Plugin Mechanism

The detectors are associated with C++ digitization routines at run time (see Fig. 8). This allows the routines to be developed independently from the core code. Abstract methods can be derived in the individual detector hit processes to define the treatment of the Geant4 steps within the detector time window to provide three kind of outputs:

- a bank with digitized variables (such as ADC, TDC) for each hit;

- a bank with digitized variables (such as ADC, TDC) for each Geant4 step;

- a bank with an analog voltage vs. time signal (such as FADC) for each Geant4 hit.

The digitized banks are detailed below for each detector subsystem.

5

Figure 8: Hit process digitization plugin association. The detectors are associated by name with the hit process routine plugins at GEMC run time. The routines are registered in the hit process map and are called during digitization.
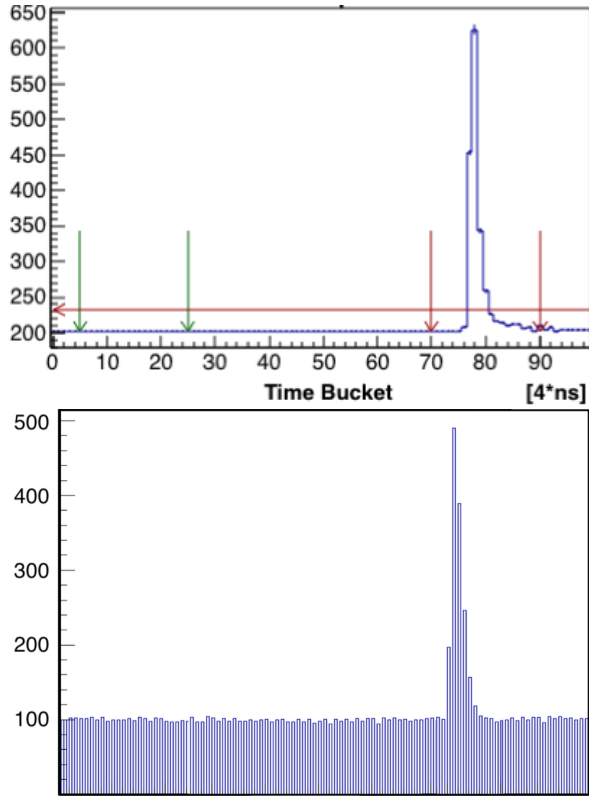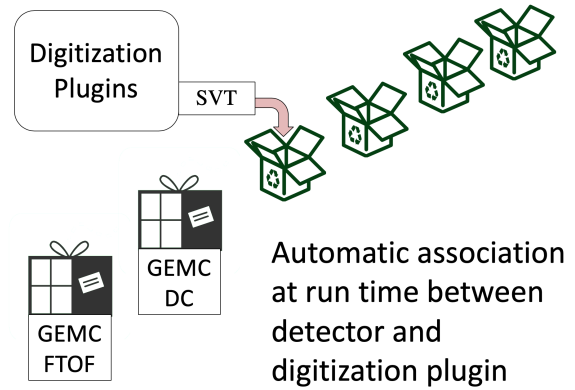
Figure 7: Top: an example of FADC digitized output as a function of sample index from the CLAS12 EC PMTs during the Spring 2018 data run. The CLAS12 DAQ system saves a 400 ns time window (100 samples, or FADC) if at least one of the 100 signal samples is above a certain threshold (horizontal line). The integral signal ADC is the sum of the output at the sample indexes between the two right arrows, one placed a few samples before the signal crosses the threshold, and the other placed a few samples after that. The pedestal is calculated using the average of the signal between the left arrows. The absolute positions of the pedestal acquisition limits and the relative position of the signal integration limits are adjusted in the DAQ parameters and loaded before each run. Bottom: the simulated EC FADC signal. The shape of the signal comes from the sum of pulse functions at each Geant4 step weighted by the energy deposited with parameters estimated from the data. These signals were used to tune the trigger system FPGA algorithms to optimize the CLAS12 trigger electronics.

1.7. "Truth" Information

Various data such as particle identification, momenta, hit positions, vertex of the particle, etc, (truth information) is stored in memory as the tracks progress in each detector. The truth information is integrated (one variable entry per GEMC hit) and/or verbose (one variable entry per Geant4 step). It is saved in the output at the end of each event. The list of variables in the truth information bank is summarized in Table 1.

1.8. Database Constants

The mechanism to read, store, and make available the calibration constants from the CLAS12 calibration constants database CCDB [25] is executed at the start of the run and every time the run number changes. The list of constants loaded is detailed in each detector implementation section below.

1.9. Digitization

The digitization routines are called at the end of each event, after the Geant4 navigation has propagated all tracks and GEMC has collected all the steps into hits.

The process routines digitize each hit by iterating through all the steps in the detector volume and collecting a number of variables into detector banks. This typically involves calculating a charge based on energy deposited and converting it into an ADC value, calculating a hit time based on various signal propagation models and converting that time into TDC, calculating the number of collected photons into charge and then ADC, etc. It is at this stage that the calibration constants are used (for example, light attenuation length in scintillator paddles).

Variable	Description
pid	ID of the FP entering the volume
mpid	ID of the mother of the FP
tid	Track ID of the FP
mtid	Track ID of the mother of the FP
otid	Track ID of the ancestor of the FP
trackE	Total energy of the FP
totEdep	Total energy deposited (in MeV)
avg_x	Average x position (in mm)
avg_y	Average y position
avg_z	Average z position
avg_lx	Average local x position
avg_ly	Average local y position
avg_lz	Average local z position
px	x of momentum of the FP (in MeV)
py	y of momentum of the FP
pz	z of momentum of the FP
vx	x of the FP's origin (in mm)
vy	y of the FP's origin
vz	z of the FP's origin
mvx	x of the FP mother's origin
mvy	y of the FP mother's origin
mvz	z of the FP mother's origin
avg_t	Average time
nsteps	Number of Geant4 steps
procID	Process that created the FP
hitn	Hit ID

Table 1: The truth information bank. The variable totEdep represents the total energy deposited (summed over all Geant4 steps within the time window). When "average" is used in the description, it refers to the mean value of all Geant4 steps within the time window. When the First Particle (FP) is indicated in the description, the variable refers only to the first (among all within the time window) Geant4 step in the sensitive element.

There are four different types of digitization, each with a different output structure:

- integrated (one bank per hit): this is implemented for all CLAS12 detectors;

- step-by-step (one bank per Geant4 step): used for debugging;

- voltage: the analog signal vs. time calculated as a response of the detector to tracks passing through it;

- fadc: the same FADC bank from crate/slot/channel as written by the CLAS12 data acquisition system [23]. This is implemented for the CND, CTOF, FTOF, FT-CAL, ECAL.

The digitization is detailed in each of the detector implementation sections below.

1.10. Output

The GEMC output is available in two formats, identical in content: text (ASCII) and EVIO [26], the Jefferson Lab data acquisition format. Utilities were used to convert the EVIO format into ROOT [27] for data analysis.

The various output banks include:

- header: time stamp, event number, run number, event type (physics event or scaler);

- generated: generated particle information as seen by Geant4. This bank includes summarized information of the interaction of the particles with each detector such as the number of hits, total energy deposited, etc. This summary includes the interactions of all created secondaries from the primary particle;

- generator extras: information stored in the generated file, not necessarily used in Geant4, for example cross sections, weights, etc.;

- beam radio-frequency signal: mimics the accelerator bank, a 248 MHz signal;

- detector truth information, per hit or per step;

- detector digitized information, per hit or per step;

- detector voltage vs. time;

- detector FADC signal;

- ancestors: the complete hierarchy of the primary and secondary particles.

The various banks are organized using a unique integer identifier.

1.11. Background Merging

Real data can be merged with simulated events, typically from random trigger data, to emulate physics and electronic backgrounds in the various detectors. The data is undigitized using the inverse digitization to calculate the energy and real timing from the ADC and TDC values. It is then saved in text files indexed by event number and detector identification (ID). This also makes it possible to scale the background luminosity by grouping several events into one; for example, grouping two events at 50 nA beam current gives one event with background from 100 nA current. The energy information is re-digitized using the same algorithm used for the Geant4 steps, producing additional hits to the ones coming from simulation.
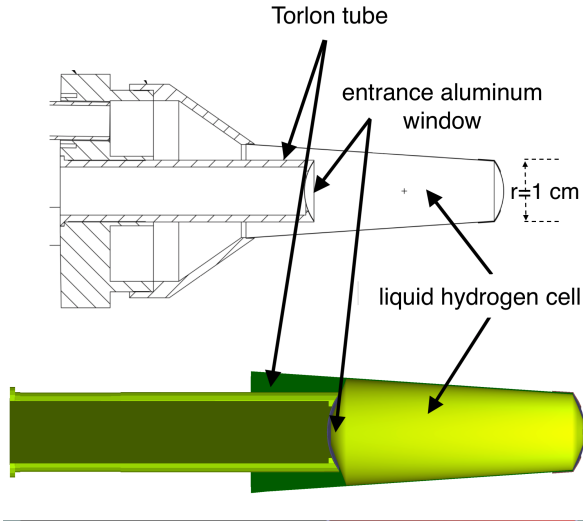
Figure 9: The CLAS12 target. Top: the engineering model of the liquid-hydrogen cell design: the outer radius is tapered down from 1.5 cm at z=-2.5 cm to 1.0 cm at z=2.5 cm (z is coordinate along the beamline). Bottom: The GEMC implementation of the CLAS12 target from the CAD drawings. From left to right (beam direction): the Torlon tube, the upstream aluminum window, the target cell, the Kapton cap, and the downstream aluminum window.

2. CLAS12 Geometry Implementation

The following sections describe the implementation of the individual CLAS12 components into the simulation.

2.1. Target

The CLAS12 target components are imported from the engineering model. The STEP files are converted to tessellated STL files and imported in the GEMC simulation [28, 29]. An example of the tessellation is shown in Fig. 4.

Key elements of the STL import include the Torlon tube to the target cell, the target aluminum windows, the Kapton walls, and the scattering chamber (see Fig. 9). An overview of the target in Geant4 and the engineering model is shown in Fig. 10.

2.2. Silicon Vertex Tracker (SVT)

The SVT [9] geometry is implemented through a JAVA service, the same used to provide the geometry to the reconstruction software [18]. This service provides the Geant4 definitions that are read by the GEMC PERL API to build the geometry database.

There are three SVT regions, with 10, 14, and 18 sectors/modules for Regions 1, 2, and 3, respectively, see
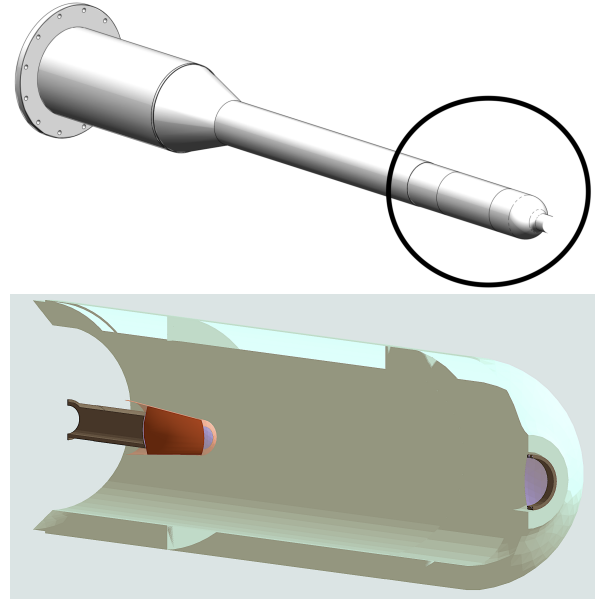

Figure 10: Top: the CLAS12 target system engineering model. This includes the support, cooling system, scattering chamber, and liquid-hydrogen cell. The circle highlights the part imported in the simulation. Bottom: overview of the target implementation in GEMC includes the foam scattering chamber (light color), the cell (also shown in Fig. 9) and, on the right, the downstream Kapton cap containing the 50 μm aluminum window.

Fig. 11. Each module has six sensors, four readout chips as passive materials, and several material components in the active area, listed in order below:

- wirebond
- silicon
- epoxy
- rail
- bus cable
- carbon fiber
- ROHACELL
- carbon fiber
- bus cable
- rail
- epoxy
- silicon
- wirebond

8

The active area of the silicon sensor is associated with the SVT hit process routine. The strip identification is performed in the Process ID routine.
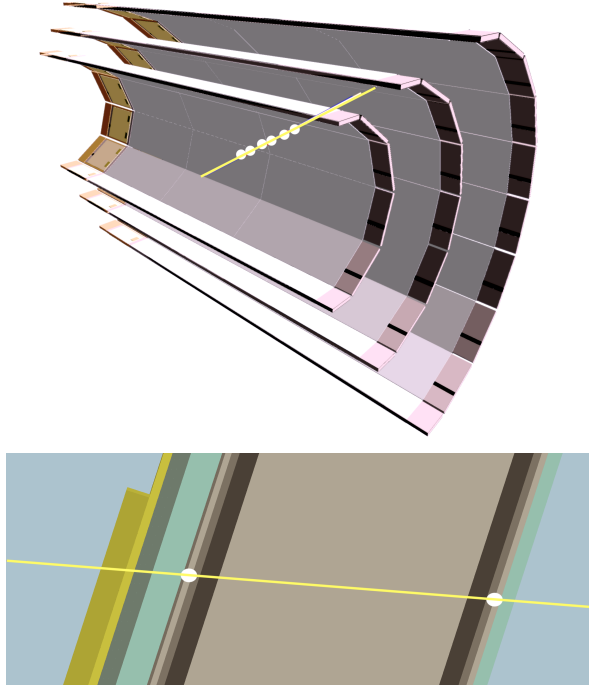

Figure 11: Top: the GEMC implementation of the SVT geometry (longitudinal cut-view). The three regions are shown in the sliced view. The silicon sensors are the gray color rectangles. The track is a 2 GeV proton, leaving hits (marked with white circles) in each sensor crossed. Bottom: detail of a module shows the various materials inside. The 320 μm silicon sensor is on inner and other surfaces of the module. The material inside includes epoxy glue, the bus cable, and support material. The proton creates one hit in both the two silicon sensors it transverses.

2.2.1. Process ID

At each Geant4 step, the local coordinates in the sensor volume are used to calculate the strip number. The algorithm includes: the dead zone around the sensor, the pitch between the readout strips (156 μm), and the angle between the strips that varies from 0° (for strip #1) to 3° (for strip #256). An illustration of the strip assignment is summarized in Fig. 12.

Due to the thickness of the silicon sensor, the produced electron avalanche can end up in more than one strip. This is reproduced in the GEMC simulation using the hit sharing algorithm described in Fig. 13.

2.2.2. Digitization

The SVT digitization provides a 3-bit ADC, using the total energy deposited (after hit sharing) between 26 and
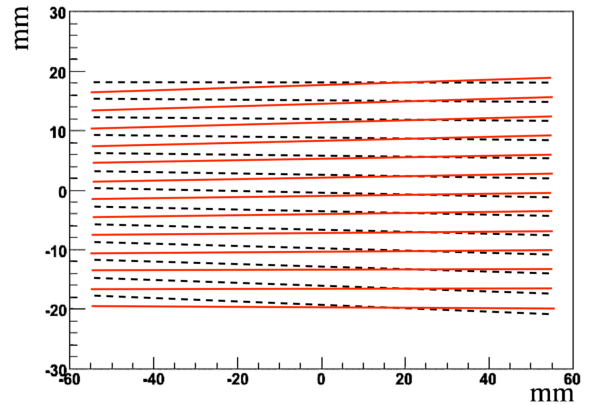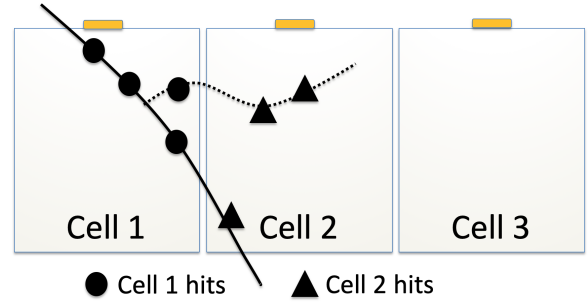

Figure 12: Top: Process ID algorithm cartoon for the SVT. The strip number is assigned based on the local position of the track step within the sensitive module. Bottom: the hit position of every 20th strip in the simulation outlines the strip boundaries. The solid and dotted distributions show the fan-like angle distributions of the strips, with opposite directions for the inner and outer layers.

117 keV. The Bunch Cross Oscillator quantity (BCO), a random number between 0 and 255, provides the TDC timing information associated with the hit. The digitized output bank variables are summarized in Table 2.

The time window of the SVT is set to to 128 ns: all Geant4 steps within the same strip and time window are collected in one hit.

2.2.3. Radiation Dose and Background Rates

A detailed study of the background rates coming from beam interacting with the target was done to ensure that the silicon sensor could operate in the high radiation conditions of the target proximity. Given the nominal operating luminosity L=10^{35} cm^{-2}s^{-1}, and the liquid-hydrogen target of 5 cm length, the beam electron rate is $R = 4.7 \times 10^{11}$ Hz. This corresponds to about 62,000 electrons in the 128 ns SVT time window.

Simulations using 62,000 11-GeV electrons per event impinging on the liquid-hydrogen target were analyzed.
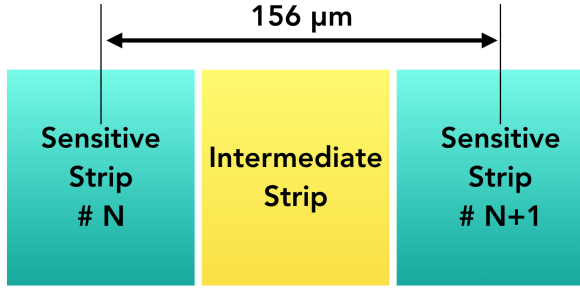
Figure 13: The SVT hit sharing algorithm. The intermediate strip represents a space between two adjacent strips used in the hit digitization algorithm. If a step happens inside the intermediate strip then 90% of its energy will be shared equally between the left and right strips (45% each), with a 10% energy loss due to capacity coupling between the strip and the back-plane.

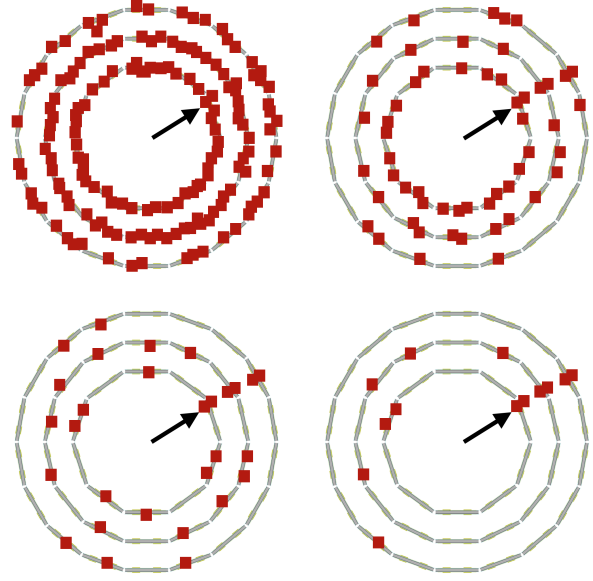| Variable	Description
layer	layer number
sector	sector number
strip	strip number
ADC	3 bit ADC
bco	8 bit time info
ADCHD	13 bit ADC
hitn	hit number

Table 2: The digitized SVT bank.

Figure 14: The occupancy in the SVT layers for different thresholds for one event containing a proton track (direction indicated by the arrow). The hits are represented by the squares. Top left: with no energy cut, all SVT layers have numerous hits. Top right: a 10 keV energy threshold reduces the SVT occupancy considerably. Most (>90%) of the hits removed come from photons. Bottom left: 20 keV energy threshold. Bottom right: 30 keV energy threshold. The SVT final choice of threshold based on the background rejection study was 30 keV.

The rates were calculated for the various regions and for different thresholds (see Fig. 14). The radiation dose and the 1 MeV neutron equivalent damage was estimated. Most of the radiation is released in the first two layers of the SVT. The 370 rad/year is low enough for an operating lifetime of at least 15 years. The results of the study are summarized in Fig. 15.

Based on these GEMC background studies in conjunction with SVT studies with beam, a thin layer of tungsten (51 μm) was added between the target and the inner SVT layer aimed at reducing the electromagnetic background [30].

2.3. Barrel and Forward Micromegas Trackers (BMT and FMT)

The BMT and FMT geometries are implemented through the native GEMC geometry API. There are two subsystems: a "barrel" Micromegas between the SVT and the CTOF, made by six concentric layers divided azimuthally in three identical sectors; and a "forward" Micromegas made in six identical disks, see Fig. 16. In the BMT, three layers have their readout strips parallel to the beam (Z strips) while the other three have them perpendicular to the beam (C strips). In the FMT, each disk (and strip orientation in a plane perpendicular to the beam) is rotated by 30° with respect to its upstream neighbor. Each elementary Micromegas detector contains a cover layer with copper ground, the printed circuit board (PCB) with the readout strips, the Kapton support, the mesh layer, the ionizing gas, and other layers of material, listed in order below:

- overlay
- copper ground
- PCB
- strips
- Kapton
- gas (amplification gap)
- mesh
- gas (drift detection gap)
- drift potential electrode
- foil

10
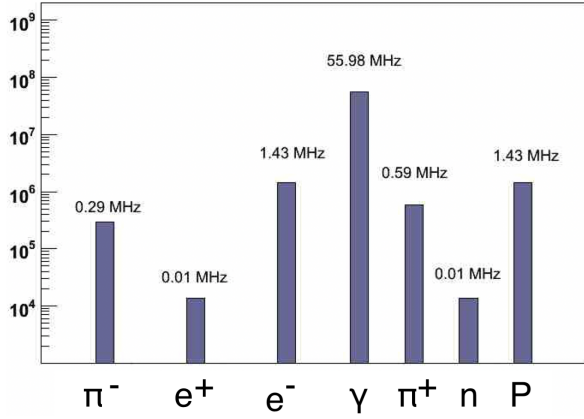
Layer	GeV/s	mrads/s	rad/year
1a	7147.8	4.39	138480
1b	3889.4	2.38	75352
2a	4578.2	0.93	29566
2b	3551.7	0.72	22936
3a	3828.5	0.34	10988
3b	3295.7	0.29	9459

Figure 15: Summary of radiation doses and background rates in the SVT. Top: the rate breakdown for different particles for a threshold of 20 keV (the current hardware threshold is 30 keV) at the full luminosity of CLAS12. Bottom: table showing the fluences and radiation doses in the SVT layers.

- ground

The sensitive volume contains argon/isobutane gas at atmospheric pressure and is associated with the BMT and FMT hit process routines. The geometry is summarized in Fig. 16. The strip identification is performed in the Process ID routine.

2.3.1. Process ID

At each Geant4 step, the local coordinates in the sensor volume are used to calculate the strip number. The algorithm includes the Lorentz angle based on the magnetic field strength, the particle direction, the pitch angle between the strips, and the dead zones of the sensitive parts. A virtual electron avalanche is simulated based on the energy deposited. The avalanche is deposited onto one strip or distributed among several to account for the energy sharing.
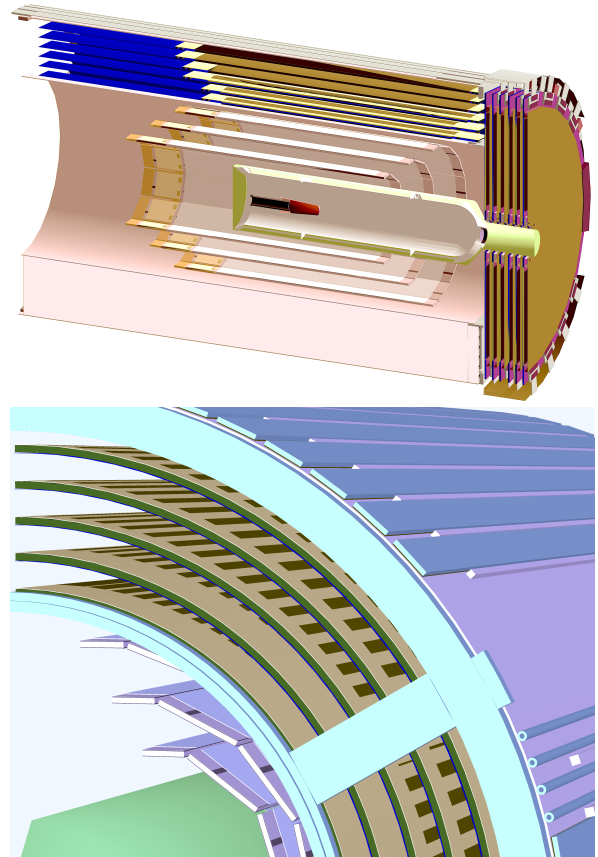

Figure 16: Top: a longitudinal cut view of the CLAS12 Central Detector trackers. The target is surrounded by 3 layers of SVT and 6 layers of Micromegas, 3 with Z-strips, 3 with C-strips. On the downstream end (beam incident from the left) the Forward Micromegas Tracker disks are visible. Bottom: detail of the Micromegas GEMC geometry, showing the overlay cover, the copper ground, and the PCB.

11

2.3.2. Digitization

The Micromegas digitization provides the ADC value calculated using the total energy deposited (after hit sharing). There is no timing information in the output. The digitized output bank variables are summarized in Table 3.

Variable	Description
layer	layer number
sector	sector number
strip	strip number
Edep	energy deposited
ADC	ADC

Table 3: The digitized BMT and FMT banks.

The time window of the Micromegas is set to to 132 ns: all Geant4 steps within the same strip and time window are collected in one hit.

2.4. Central Time-Of-Flight (CTOF)

The CLAS12 CTOF paddles and light guides (see Fig. 17 top) are imported from the engineering model. The STEP files are converted to tessellated STL files and imported directly into the GEMC simulation [31]. The STL files are downloaded using the JAVA geometry service, as the same files are used in reconstruction. The paddles are assigned the scintillator material and associated with the CTOF hit process routine. The light guides are also associated with the scintillator material, but they are treated as passive material and not associated with a sensitive detector.

Each volume is typically tessellated by about 1,000 facets. The simulation geometry captures complicated details such as the shape of the scintillator/light guide junctions, see Fig. 17 bottom.

2.4.1. Process ID

Each hit in the paddles produces two hits with the identifier variable "side" set to 0 (for the upstream PMT) and 1 (for downstream PMT). The hits are then processed independently through the CTOF hit process routine.

2.4.2. Digitization

The energy deposited is reduced based on the hit position on the paddle using the calibrated light attenuation length. It is then corrected by a gain factor to account for the fact that the high voltages (HVs) are adjusted so that the average upstream/downstream ADC geometric mean is independent of hit position.
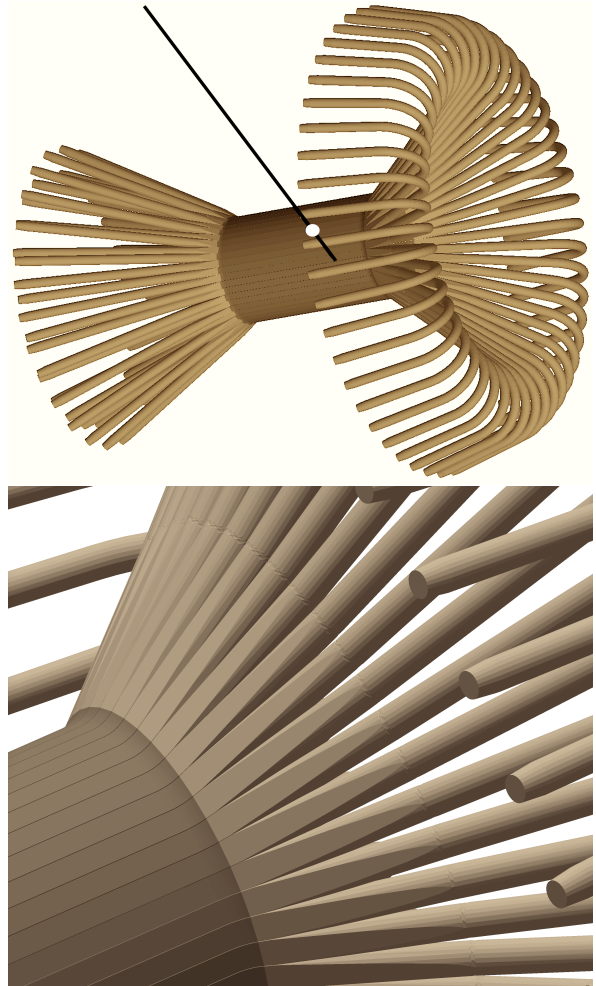

Figure 17: Top: the GEMC implementation of the CTOF geometry. Beam is incident from the left. The paddles and light guides are imported directly from the engineering model. The black line is a 2 GeV proton leaving a hit (white circle) in one of the paddles. Bottom: a zoom-in of the implementation shows the details of downstream scintillator/light guide junctions: the scintillator bends near the junction, the light guide starting with the trapezoidal counter shape, and morphing into a circular cross section.

The corrected energy is converted to the data derived number of photons N_{th} using the constant 500 γ/MeV. A Poissonian distribution is used to calculate the actual number of photons N_{actual} and the resulting "smeared" energy is converted to ADC using the FADC conversion factor.

The absolute hit time is corrected using calibration constants estimated from data:

- the effective velocity;

- an upstream/downstream PMT time offset factor;

- an RF correction.

The time is then smeared by a resolution read from CCDB using a Gaussian function and then digitized using a TDC conversion factor. The digitized output bank variables are summarized in Table 4. Note there is no time-walk correction for the measured CTOF times as constant fraction discriminators are employed for the readout.

Variable	Description
sector	sector number
layer	layer
paddle	paddle number
side	0 upstream, 1 downstream
ADC	ADC
TDC	TDC
ADCu	ADC unsmeared
TDCu	TDC unsmeared
hitn	hit number

Table 4: The digitized CTOF bank.

The time window of the CTOF is set to to 400 ns: all Geant4 steps within the same paddle and time window are collected in one hit.

2.5. Central Neutron Detector (CND)

The CND geometry is implemented through the native GEMC geometry API. The paddles are Geant4 generic trapezoids (see Fig. 18). The U-turn light guides are Geant4 "polycones" (volumes with cylindrical symmetry with varying radius along one axis). The paddles are assigned the scintillator material and associated with the CND hit process routine.
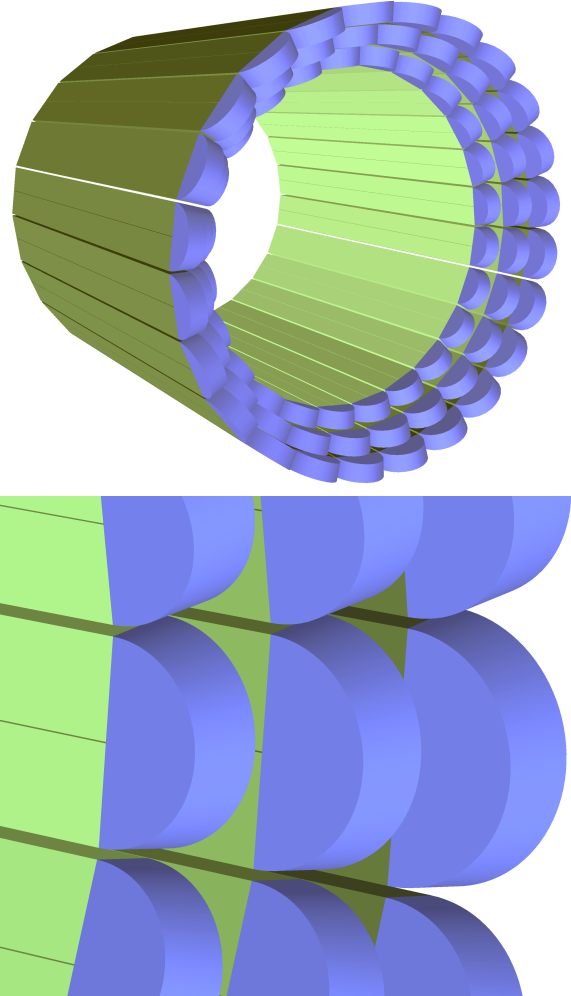

Figure 18: Top: overall view of the CND detector. Beam is incident from the left. Three layers of scintillator are placed at increasing z. Pairs of scintillators are connected through a scintillator u-turn junction. Bottom: enlarged view of the junctions.

13

2.5.1. Digitization

The energy deposited is reduced based on the position in the paddle using the calibrated light attenuation length. Two signals are then propagated, one to the PMT attached to the scintillator ("direct hit"), and one traveling through the scintillator junction onto the other scintillator and its PMT ("indirect hit"). Layer-dependent factors, applied to the two signals, account for the light loss in the U-turn and in the neighboring paddle. These factors were determined during cosmic-ray tests.

The corrected energy is converted to the theoretical number of photons N_{th} using the constant 1210 γ/MeV, which accounts for light propagation in the 1.4-m-long light guides, for losses at the junctions and for the quantum efficiency of the PMT. A Poissonian distribution is used to calculate the actual number of photons N_{actual} and the resulting "smeared" energy is then converted to ADC using the FADC conversion factor.

The absolute hit time is corrected using calibration constants estimated from data:

- the effective velocity;

- a left/right time offset factor;

- the Birks-attenuation factor;

- the position and corresponding paddle length of the direct and the indirect hit.

The time is then smeared by a resolution read from CCDB using a Gaussian function and then digitized using a TDC conversion factor. The Birks factor, reducing the deposited energy depending on the particle type, enters in the timing calculation as follows: the direct and indirect times are smeared with a Gaussian function having a width directly proportional to an empirically determined constant, and inversely proportional to the square root of the measured light (which is, in turn, proportional to the attenuated energy). The digitized output bank variables are summarized in Table 5.

The time window of the CND is set to 400 ns: all Geant4 steps within the same paddle and time window are collected in one hit.

2.6. High Threshold Cherenkov Counter (HTCC)

The HTCC geometry is implemented through the native GEMC geometry API. The elliptical mirrors are subtractions of ellipsoid Geant4 volumes along certain planes between two adjacent mirror substrates. Each plane is defined by a second-order curve along which the two substrates intersect. They are contained inside an HTCC mother volume made with a Geant4 "polycone" (see Fig. 19). The faces of the PMTs are the sensitive volumes, associated with the quartz-glass material and with the HTCC digitization routine.

The refractive index of the CO_2 radiator gas and its transparency is included in the material optical properties and taken into account during the Geant4 transportation of the photons. The same is true for the reflectivity of the mirrors and Winston cones. Finally, the quantum efficiency associated with the PMT photo-cathode is taken into account in the digitization routine.

2.6.1. Digitization

Photons that impinge on the PMT faces are processed with the digitization routine. Each photon collected is input to the quantum efficiency algorithm at its wavelength to decide if it is finally detected.

The time average of all the photons is saved in the output after a time shift coming from the calibration database. The digitized output bank variables are summarized in Table 6.

Variable	Description
sector	sector number
layer	layer number
component	component number
ADCL	ADC Left
ADCR	ADC Right
TDCL	TDC Left
TDCR	TDC Right
hitn	hit number

Table 5: The digitized CND bank.

Variable	Description
sector	CLAS12 sector
ring	theta index
half	half-sector
nphe	number of photo-electrons
time	average time of the hit
hitn	hit number

Table 6: The digitized HTCC bank.

The time window of the HTCC is set to 5 ns: all Geant4 steps within the same PMT and time window are collected in one hit.

2.7. Forward Tagger (FT)
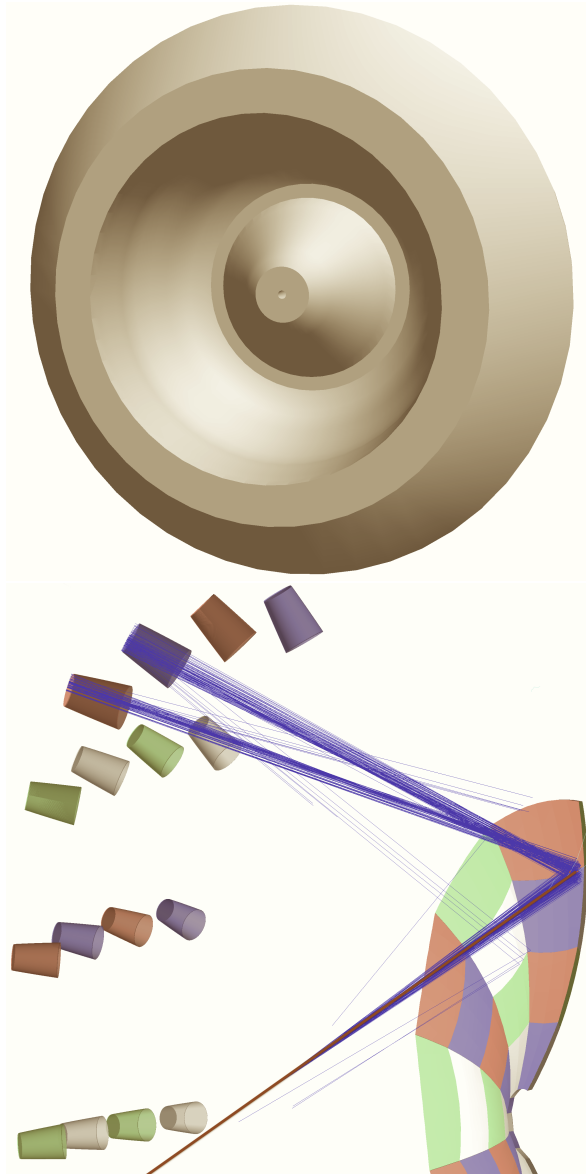
The FT consists of three subsystems:

- a tracker (FT-Trk), composed by 4 micromegas layers;

- a hodoscope (FT-Hodo), with eight sectors, each containing two layers of scintillators;

- a calorimeter (FT-Cal) containing an array of 332 crystals.

The three subsystems are implemented in GEMC using the native PERL API script, except for the inner shield (see Section 2.14), which comes from the CAD engineering model. The FT geometry is shown in Fig. 20.

2.7.1. Digitization

The FT-Trk digitization provides the ADC value calculated using the total energy deposited (after hit sharing). There is no timing information in the FT-Trk output.

For FT-Cal hits, the energy deposited is converted first to the charge produced at the end of the electronics chain composed by an avalanche photodiode (APD) and preamplifier, and then to an ADC. The first conversion is based on the measured charge for cosmic rays that deposit a known energy in the crystals, while the second conversion is based on the FADC conversion factor. A smearing on the final ADC values is added, accounting for the Poisson distribution of photoelectrons produced by the photosensor, the Gaussian noise of the photosensor, and of the preamplifier. All parameters, the number of photoelectrons per MeV of energy deposited, the RMS width of the APD noise, and of the preamplifier input noise, have been tuned to the experimental data.

The same approach is adopted to process FT-Hodo hits. The output is read by silicon photomultipliers (included in the simulation) in which the deposited energy is first converted to charge and then to ADC. The smearing in this case accounts only for the Poisson distribution of the measured number of photoelectrons, which dominates over other sources because of the relatively small number of photoelectrons per MeV of energy deposition.

The TDC of FT-Cal hits is computed from the time of the energy deposition, accounting for the speed of the scintillation light in the crystal and the distance to the photo-sensor, assuming a known time-to-TDC conversion factor. A Gaussian smearing on the resulting TDC is added based on a fixed RMS resolution derived from the experimental measurements.

Similarly, the TDC of FT-Hodo hits is derived from the time of a given energy deposition, adding a fixed offset before the conversion from time to TDC and a Gaus-

Figure 19: Top: the upstream side of the HTCC containment vessel. Bottom: an electron passing through the HTCC gas volume and emitting Cherenkov photons. The light cone hits two mirrors and it is re-directed to the corresponding PMTs.

15

FT-HODO

FT-CAL

FT-TRK electronics
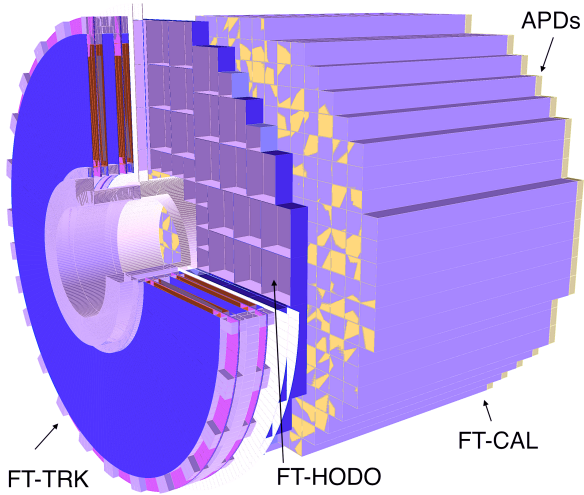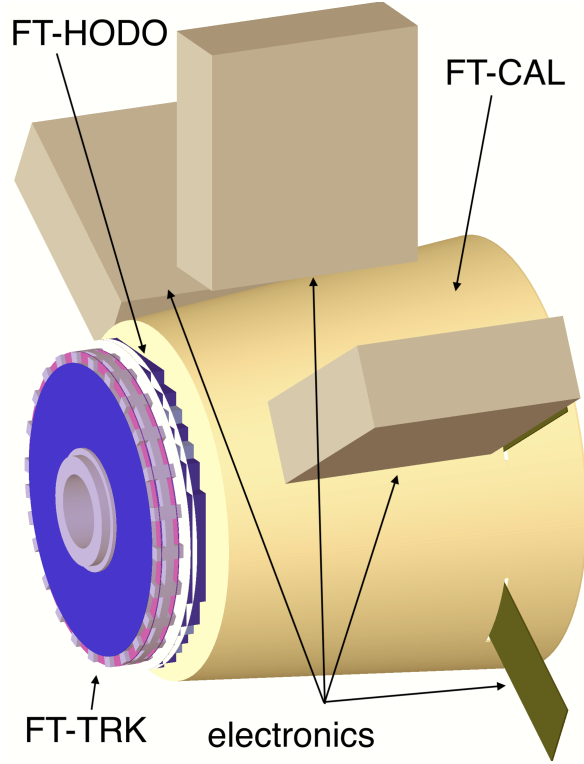
APDs

FT-CAL

FT-TRK FT-HODO

Figure 20: Top: the FT detector implementation in GEMC. The boxes surrounding FT-Cal contain the electronics. Bottom: details of the implementation of the three subsystems. As seen by the beam (incident from the left): the disks form the FT-Trk; the FT-Hodo scintillators just behind the tracker; and the FT-Cal crystals.

sian smearing. As in previous cases, all relevant parameters have been tuned to the observed detector response. The digitized output bank variables are summarized in Table 7.

Variable	Description
	Tracker
layer	tracker layer
component	strip number
ADC	ADC
	Hodoscope
sector	hodoscope sector
layer	hodoscope layer
component	tile number
ADC	ADC
TDC	TDC
	Calorimeter
component	crystal number
ADC	ADC
TDC	TDC

Table 7: The digitized FT banks for the tracker, hodoscope, and calorimeter.

The time window of the tracker is set to to 132 ns: all Geant4 steps within the same strip and time window are collected in one hit. The time window of the hodoscope and calorimeters are set to 400 ns: all Geant4 steps within the same paddles and time window are be collected on one hit in each system.

2.8. Drift Chambers (DC)

The DC geometry is implemented through the JAVA geometry service. The service provides the Geant4 definitions that are read by the GEMC PERL API to build the geometry database.

For each of the six sectors of the CLAS12 Forward Detector, there are three drift chambers: one in front of the torus magnet, one between the torus coils, and one after the torus. These three chambers are referred to as different "regions". The chambers are strung with the wires arranged in 12 internal layers. Each layer is a generic G4Trapezoid, tilted by +6° or -6° depending if they are in the first or second "superlayer" of a region. The 12 layers in each region (6 per superlayer) are placed in a region mother volume made of air (see Fig. 21). The layers are assigned the DC gas mixture: 90% argon/10% CO_2. Each layer is associated with the DC hit process routine. The hit wire identification is performed in the Process ID routine.
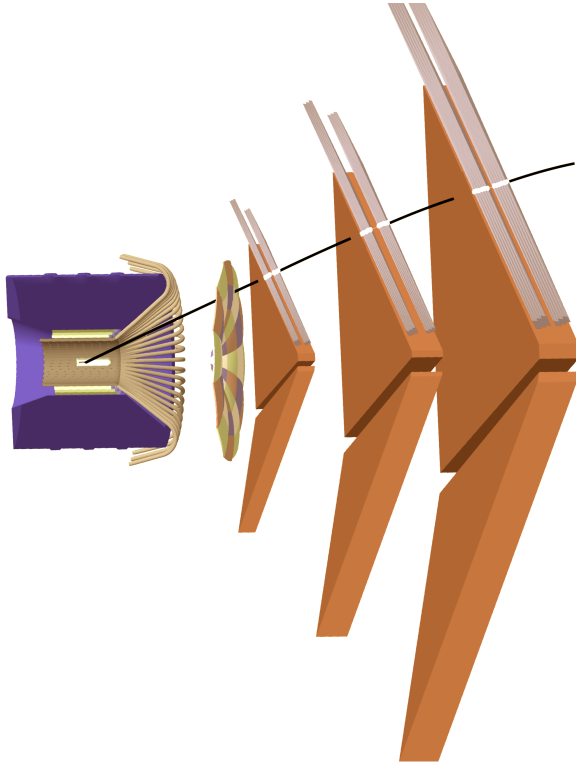
16

Figure 21: The GEMC implementation of the DC geometry (longitudinal cut-view). Beam is incident from the left. The solenoid magnet volume, CTOF, CND, and HTCC are also visible. Geant4 trapezoids are the mother volumes corresponding to DC Regions 1, 2, and 3. The track is a negative pion, hitting the various layers inside each region. The hits are indicated by the white markers. Due to the high DC efficiency, most tracks produce at least one hit in each layer (12 hits/region). The wire hit inefficiencies are incorporated in the simulation parameters to match the experimental data.

2.8.1. Process ID

The wire number is calculated using the formula $n_i = y/\delta y$, where y is the distance from the center of the DC layer trapezoid volume projected along its vertical axis and δY is the distance between each wire. The wire sagging due to gravity and mechanical deflections of the wire endplates due to the tension load are not taken into account.

2.8.2. Digitization

First, the distance of closest approach of the passing track to the hit wire (*DOCA*) is computed for the hit in each layer. At each Geant4 step, the distance of the track from the wire is calculated. The *DOCA* is extracted among the points with energy deposited larger than 50 eV, for which the sum of the step time + *DOCA*/drift velocity is minimal.

An initial time T_i is calculated with a time-to-distance

function that is the inverse of what is determined from calibration and used in reconstruction to go from TDC to *DOCA*. The function takes into account:

- the distance from the wire, in cm;
- the cell size in each superlayer;
- the polar angle of the track;
- magnitude of the torus field.

A time-walk correction function T_w is applied to T_i that includes discrete ionization effects based on the following input:

- the distance from the wire, in cm;
- the cell size in each superlayer;
- the velocity of the particle;
- an overall parameter to adjust to data at small distances from the wire.

The resulting T_w is then used in a Landau function to mimic the detector response function.

An intrinsic random time-walk correction σ_{TW} due to multiple scattering is calculated and the time is smeared with a Gaussian function using σ_{TW} as the resolution. A random number is thrown (between 0 and 1) and if it is above the efficiency function calculated based on *DOCA*, the hit is rejected. Finally, the timing is smeared using the calibrated residual vs. *DOCA* function (see Fig. 22).

The digitized output bank variables are summarized in Table 8.

Variable	Description
sector	sector index
layer	layer index
wire	wire index
TDC	tdc value
LR	Left/Right ambiguity
doca	2D distance of closest approach
sdoca	smeared doca
time	DOCA/drift velocity
stime	smeared DOCA/drift velocity

Table 8: The digitized DC bank.

The simulation time window of the DC is set to 500 ns: all Geant4 steps within the same cell and time window are collected in one hit. The actual readout electronics time windows are set to 250, 500, and 750 ns for Regions 1, 2, and 3, respectively.
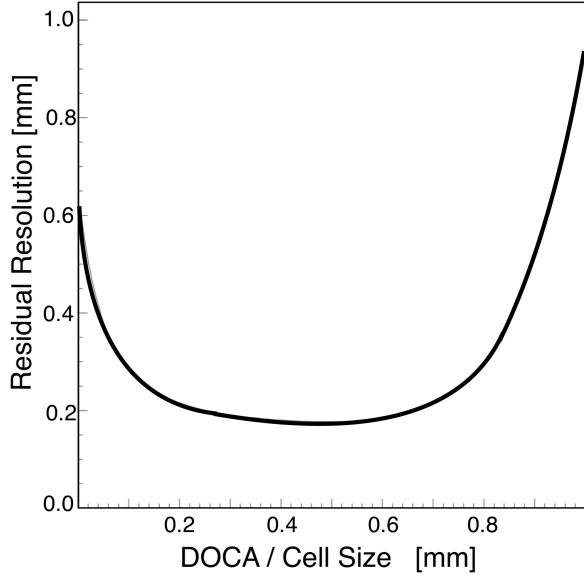
Figure 22: The fit to the DC data resolution provides parameters that are put in the CCDB database and read by the digitization routine at simulation run time.

2.8.3. Background Rates

A detailed study of the background rates coming from beam interacting with the target was done to ensure that the DC occupancy stays within limits that do not affect the track reconstruction efficiency, typically below 5%.

Given the operating luminosity L=10^{35} cm^{-2}s^{-1}and the liquid-hydrogen target length of 5 cm, the beam electron rate is R=4.7×10^{11} Hz. This corresponds to around 124,000 electrons in the DC 250 ns time window of Region 1.

Various analyses [29, 32, 33], were performed using 124,000 electrons/event to study the DC occupancy response to variations of hardware position and beamline configurations. The rates were scaled in Region 2 and 3 to take into account the difference between the real and simulated time window. The results are summarized in Fig. 23. The highest DC occupancy is in Region 1. The source is mostly electromagnetic background from the target and beamline elements. Regions 2 and 3 are shielded against leptons by the torus magnetic field. Region 3 is exposed to radiation coming from the interactions of the broadened beam (due to interactions in the target) with the torus components (especially the most downstream elements). In general, the occupancy in the DC affects the track reconstruction efficiency. A value of 3% occupancy in Region 1 is considered an optimal compromise between luminosity and reconstruction efficiency [18].
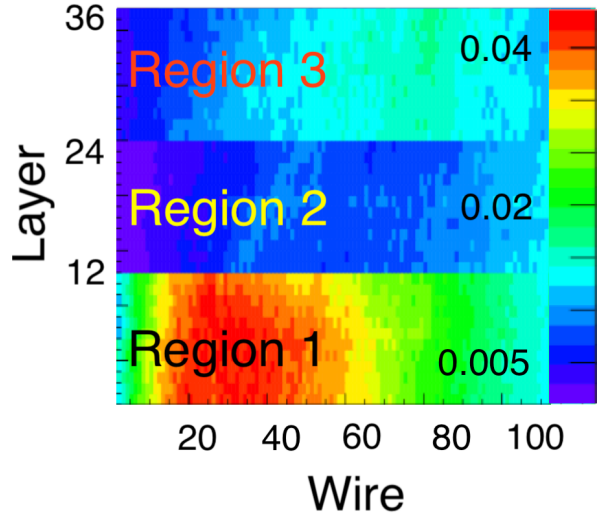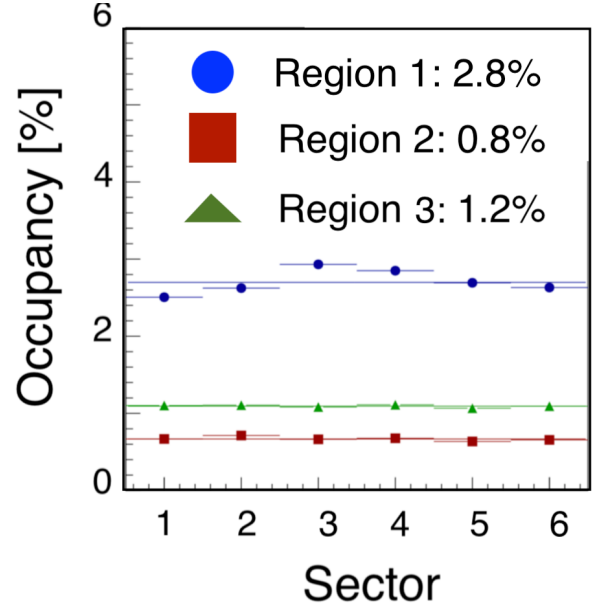

Figure 23: Results for DC rates for electrons outbending in the torus field. Top: the occupancy is below 3% for Region 1 and 1.2% for Region 3. Bottom: layer vs. wire hit distribution. Results for the electron inbending polarity shows very similar distributions.

18

2.9. Low Threshold Cherenkov Counter (LTCC)

The LTCC mirror geometry is implemented through the native GEMC geometry API. The elliptical mirrors are made through a subtraction of two ellipsoids. The hyperbolic mirrors are built using Geant4 "polycones" approximating the mathematical shape using about 30 segments. The cylindrical mirrors are made from cuts of cylinder volumes.

The LTCC Winston cones (WCs) are of three types: small, medium, and large. Three CAD models are tessellated and imported in the simulation, and then copied into 36 WCs/sector using the PERL API.

Finally, the LTCC box, mirror support structure, and additional support hardware are imported directly from the engineering CAD models. Figure 24 shows details of the geometry implementation.

The refractive index of the C_4F_{10} radiator gas and its transparency is included in the material optical properties and taken into account during the Geant4 transportation of the photons, as is the reflectivity of the mirrors and Winston cones. The quantum efficiency associated with the PMT photocathodes is taken into account in the digitization routine.

2.9.1. Digitization

Photons that impinge on the PMT faces are processed with the digitization routine. Each photon collected is input to the quantum efficiency algorithm at its wavelength to decide if it is detected. The ADC energy is calculated and smeared using the single photoelectron peak position and width from the calibration database. The time average of all the photons is saved in the output. The digitized output bank variables are summarized in Table 9.

Variable	Description
sector	CLAS12 sector
side	left or right index
segment	segment
ADC	ADC
time	average time of the hit
nphe	number of photons at the PMT face
npheD	number of photons at the electronics
hitn	hit number

Table 9: The digitized LTCC bank. The digitization takes into account the PMT quantum efficiency to derive the number of photons at the electronics (photons detected) from the photons hitting the face of the PMT.

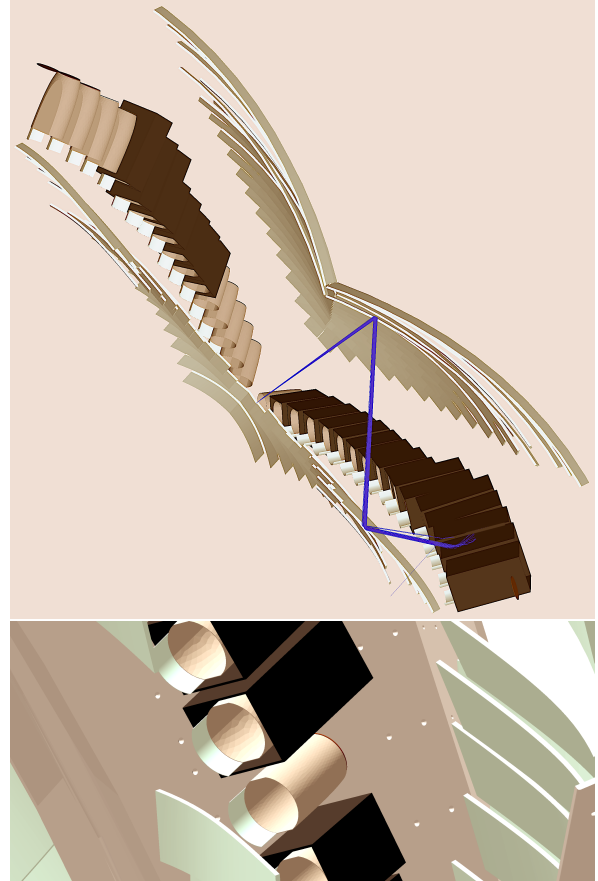The time window of the LTCC is set to 50 ns: all

Figure 24: Top: a 6 GeV pion passing through the LTCC gas volume and emitting Cherenkov photons. The light cone bounces from the elliptical to the hyperbolic mirrors to the WC, and finally reaches the PMT. Bottom: details of the hardware inside the LTCC simulation system: the box frame and the WC are imported from CAD. The mirrors, magnetic shields, and PMTs are made with Geant4 volumes. One of the PMT magnetic shields in this picture was removed to show the WC. The PMT is simulated as a disk attached to the WC.

Geant4 steps within the same PMT and time window are collected in one hit.

2.10. Ring-Imaging Cherenkov (RICH)

One of the six CLAS12 Forward Carriage sectors has been equipped with a Ring Imaging Cherenkov detector [6].

The RICH mirror geometry is implemented through both the native GEMC geometry API and imports from the engineering model STEP files. The spherical mirrors are made through Geant4 boolean intersections of spheres and planes. Since the array of 391 PMTs is inside the CLAS12 acceptance, particular care went into implementing in the simulation the details of the PMT hardware and materials: the PMTs are Geant4 aluminum boxes containing the electronic components materials (accounting for the adapter, the multi-anode readout chip, and FPGA boards), the window, and the photocathodes. Each multi-anode PMT contains 64 pixels. The identification of the pixel is done in the process identification routine. The aerogel radiator tiles are imported from the engineering CAD models and include the triangular, squared, pentagonal, and trapezoidal shapes. The RICH box, mirror support structure, tile wrapping, planar mirrors, and additional support hardware are also imported from the engineering CAD models. Figure 25 shows details of the geometry implementation.

The refractive index and transparency was measured for each aerogel tile, and is included in the simulation by assigning a unique material to each aerogel volume with the proper optical properties, as is the reflectivity of each of the spherical and planar mirrors. The quantum efficiency associated with the PMT photocathodes is taken into account in the digitization routine.

2.10.1. Process ID

At each Geant4 step, the local coordinates in the PMT volume are used to calculate the pixel number within that PMT.

2.10.2. Digitization

Photons that impinge on the PMT faces are processed with the digitization routine. Each photon collected is input to the quantum efficiency algorithm at its wavelength to decide if it is detected. The total number of photoelectrons is then calculated based on the PMT gains and the calibrated response. Finally, algorithms based on the calibration parameters from CCDB are used to determine the leading and trailing edge times, which are then converted to TDCs. The digitized output bank variables are summarized in Table 10.
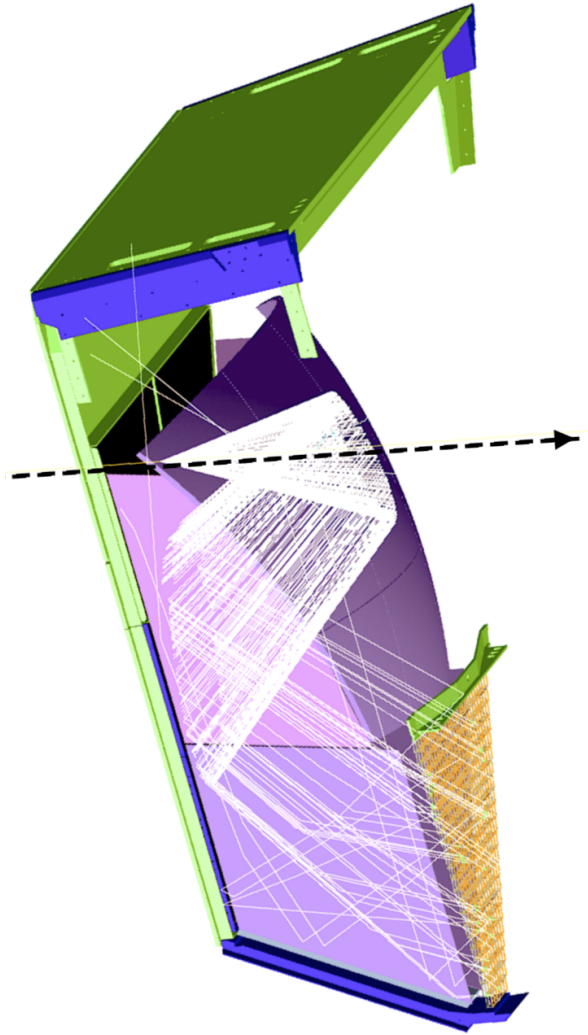

Figure 25: The implementation of the RICH geometry. Beam is incident from the left. A 4 GeV kaon produces a Cherenkov light cone. Part of the cone reflects onto the spherical mirror and into the PMT array. The remaining photons go through the aerogel tiles and bounce off the planar mirror onto the PMT array. All inefficiencies are taken into account by using the aerogel refractive index and its transparency.

20

Variable	Description
sector	CLAS12 sector
pmt	PMT number
pixel	pixel number within the PMT
TDCL	TDC leading edge
TDCT	TDC trailing edge
time	average time of the hit
nphe	number of photons at the PMT face
npheD	number of photons at the electronics
hitn	hit number

Table 10: The digitized RICH bank. The digitization takes into account the PMT quantum efficiency to derive the number of photons at the electronics (photons detected) from the photons hitting the face of the PMT.

The time window of the RICH is set to 300 ns: all Geant4 steps within the same PMT pixel and time window are collected in one hit.

2.11. Forward Time-Of-Flight (FTOF)

The FTOF geometry is implemented through the JAVA geometry service. The service provides the Geant4 definitions that are read by the GEMC PERL API to build the geometry database.

Each scintillator is a separate Geant4 volume. The paddles are assigned the scintillator material and associated with the FTOF hit process routine. Each scintillator is a box volume embedded in a trapezoidal mother volume made of air (see Fig. 26).

2.11.1. Process ID

Each hit in the paddles produces two hits with the identifier variable "side" set to 0 (for the left side PMT) and 1 (for right side PMT). The hits are then processed independently through the FTOF hit process routine.

2.11.2. Digitization

The energy deposited is reduced based on the hit position on the paddle using the calibrated light attenuation length. It is then corrected by a gain factor to account for the fact that the high voltages (HVs) are adjusted so that the average left/right ADC geometric mean is independent of counter length and hit position.

The corrected energy is converted to the number of photons N_{th} using the constant 500 photons/MeV, which was estimated from data. A Poissonian distribution is used to calculate the actual number of photons N_{actual} and the resulting "smeared" energy is the converted to ADC using the FADC conversion factor. An example of
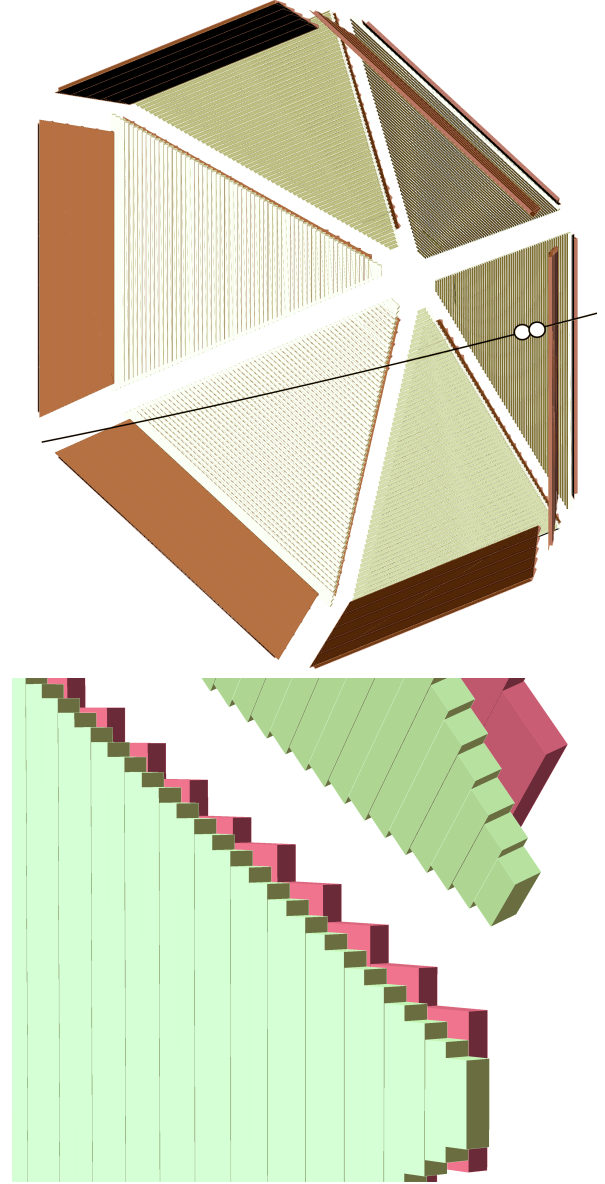

Figure 26: Top: the GEMC implementation of the FTOF geometry. Beam is incident from the left. The paddles are G4Boxes embedded in trapezoids representing the mother volumes of each panel. A 6 GeV pion is shown, producing one hit (white circle) in each FTOF panel in the CLAS12 Forward Detector Sector 4. Bottom: a zoom-in of the implementation shows the details of the individual paddles for panel-1b (upstream, in front) and panel-1a (downstream).
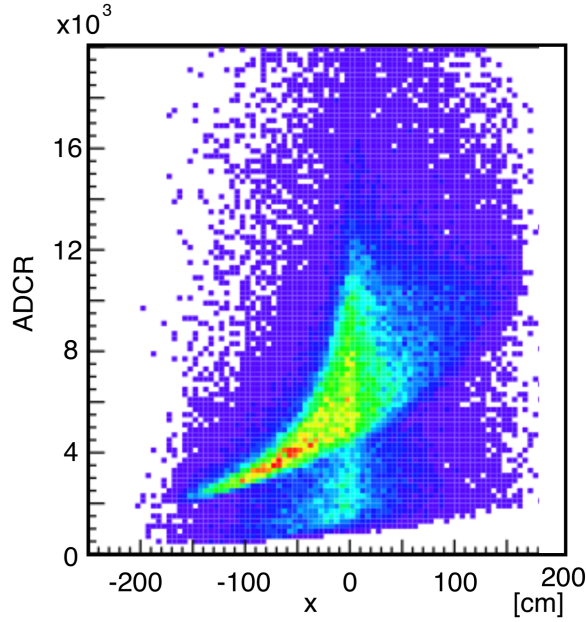
Figure 27: The ADC of the FTOF right paddle PMTs as a function of the relative position of the hit in the paddle. The effects of attenuation length and smearing using realistic constants from the CCDB database make the FTOF simulation response very similar to the real data.

the smeared ADC for the right paddles as a function of hit position is shown in Fig. 27.

The absolute hit time is corrected using calibration constants estimated from data:

- the effective velocity;

- the time-walk correction, calculated from the smeared energy;

- a panel-to-panel timing offset factor;

- a left/right time offset factor;

- an RF correction.

The time is then smeared by a resolution read from CCDB using a Gaussian function and then digitized using a TDC conversion factor. The digitized output bank variables are summarized in Table 11.

The time window of the FTOF is set to 400 ns: all Geant4 steps within the same paddle and time window are collected in one hit.

2.12. Electromagnetic Calorimeter (EC) and Pre-Shower Calorimeter (PCAL)

Both the EC and PCAL (referred to together as ECAL) calorimeter geometry is implemented through

Variable	Description
sector	sector number
layer	layer (1: 1a, 2: 1b, 3: 2)
paddle	paddle number
side	PMT side (0 Left, 1 Right)
ADC	ADC
TDC	TDC
ADCu	ADC unsmeared
TDCu	TDC unsmeared
hitn	hit number

Table 11: The digitized FTOF bank.

the JAVA geometry service. The service provides the Geant4 definitions that are read by the GEMC PERL API to build the geometry database.

Each scintillator is a separate Geant4 volume. The paddles are assigned the scintillator material and associated with the ECAL hit process routine. Each scintillator is a trapezoid embedded in a trapezoidal mother volume made of air (see Fig. 28).

2.12.1. Digitization

The digitization is the same for both the EC and the PCAL calorimeters. The energy deposited is reduced based on the position on the scintillator using the calibrated light attenuation length. The number of photons N_γ produced in the scintillator is derived from this energy using a Poissonian distribution. N_γ is then smeared using the scintillator resolution σ_{res} estimated from the data. Fluctuations in the PMT gains, also estimated from data, are also applied to N_γ and a conversion factor is used to produce an ADC output.

The absolute hit time is corrected using the light attenuation length and an additional factor that accounts for the time-walk correction. The digitized output bank variables for both systems are summarized in Table 12.

Variable	Description
sector	sector number
stack	scintillator layer number
view	view
strip	strip number
ADC	ADC
TDC	TDC
hitn	hit number

Table 12: The digitized EC and PCAL banks.

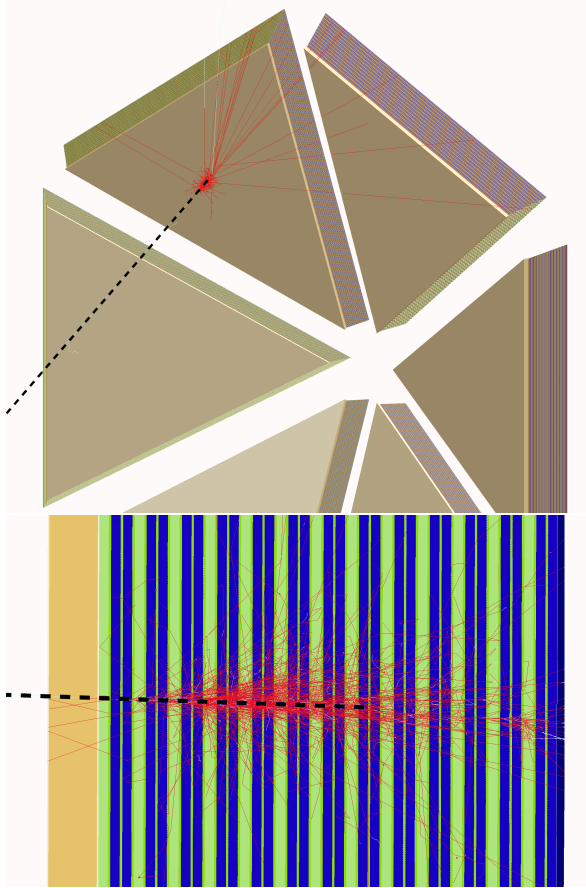The time window of both the PCAL and EC is set

to 400 ns: all Geant4 steps within the same paddle and time window are collected in one hit.

2.13. Solenoid and Torus Magnets

The solenoid magnet geometry is produced with the GEMC PERL API. The solenoid is a single Geant4 polycone volume, shown in Fig. 29.
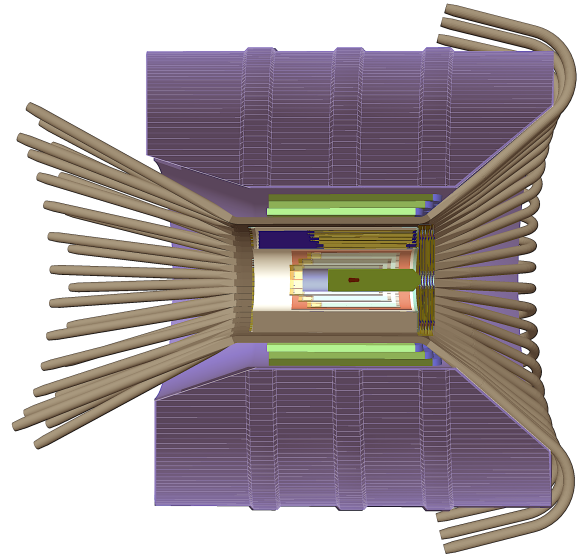

Figure 29: A cut-out of the CLAS12 Central Detector showing the solenoid volume around it. Beam is incident from the left.

The torus magnet geometry is imported from the engineering CAD model through 54 tessellated volumes. Among the volumes are:

- the bore heat shield and hub components;

- the back and front hub steel plates;

- the stainless steel coil vacuum jackets;

- the torus coils containing the conductors, represented by copper volumes in Geant4;

- internal shielding around the hub, made by tungsten cylinders (blue in Fig. 30).

The torus hub is protected from the beam pipe background with additional tungsten shielding. The torus geometry is shown in Fig. 30.

2.13.1. Magnetic Field Maps

The CLAS12 torus and solenoid field maps are imported into the simulation using ASCII files. Both fields can be scaled by an arbitrary factor. Both fields are defined in the Hall-B coordinate system and both can be shifted and tilted by additional small amounts.

Figure 28: Top: a 4 GeV electron track (dotted line) showering in the GEMC implementation of the ECAL geometry. Beam is incident from the left. The scintillator layers alternate with a layer of lead, for a sampling fraction of about 0.3. Bottom: a zoom-in transverse view of the electron shower.

23

2.13.2. Solenoid

The solenoid field map has cylindrical symmetry around the z-axis (beamline), so the map used in the simulation is defined in the transverse/longitudinal plane and then rotated when requested by the Geant4 navigation. The integration method used in the simulation is the fourth-order Runge-Kutta technique [22].

The field map grid size is based on measured field variations and uniformity. The grid is made by 600 points in the transverse coordinate, from 0 to 3 m and by 1200 points along the z-axis, from -3 m to 3 m. The field grid values are linearly interpolated to the (x, y, z) coordinate requested by Geant4. Table 13 shows the field map ASCII data structure. The simulation of one event in a 250 ns time window at the CLAS12 luminosity with and without solenoid magnetic field is presented in Fig. 31, showing the effectiveness of the solenoid in providing electromagnetic shielding of Møller electrons.

T (m)	Z (m)	B_T (T)	$B_L(T)$
0.005	-0.025	0.000013	5.000880
0.005	-0.020	0.000044	5.000822
0.005	-0.015	0.000073	5.000704
0.005	-0.010	0.000101	5.000529
0.010	-0.025	0.000028	5.000928
0.010	-0.020	0.000089	5.000867
0.010	-0.015	0.000148	5.000747
0.010	-0.010	0.000203	5.000570

Table 13: Solenoid ASCII field map values around the target. T is the transverse coordinate $\sqrt{(x^2 + y^2)}$ and z is the longitudinal coordinate. The solenoid field is centered at $z = 0$, the location of the center of the target. These values refers to the target location, where the field is designed to be constant. The map includes the complex geometric fall-off of the fringe field in the exit to the bore.

2.13.3. Torus

The torus field can be imported using a symmetric map or a full 3D map. The symmetric map is defined in half of a CLAS12 sector. It is symmetric around the sector midplane and copied in each sector when requested by the Geant4 navigation. The 3D map covers the entire Cartesian space and accounts for field deviations due to coil movements or imperfections [34].

The field map has 251 points along the z-axis from 1 m to 3 m. It has 2501 points in the transverse coordinate from 0 to 5 m. It has 16 azimuthal points from 0° to 30°. The field grid values are linearly interpolated to the (x, y, z) coordinate requested by Geant4.
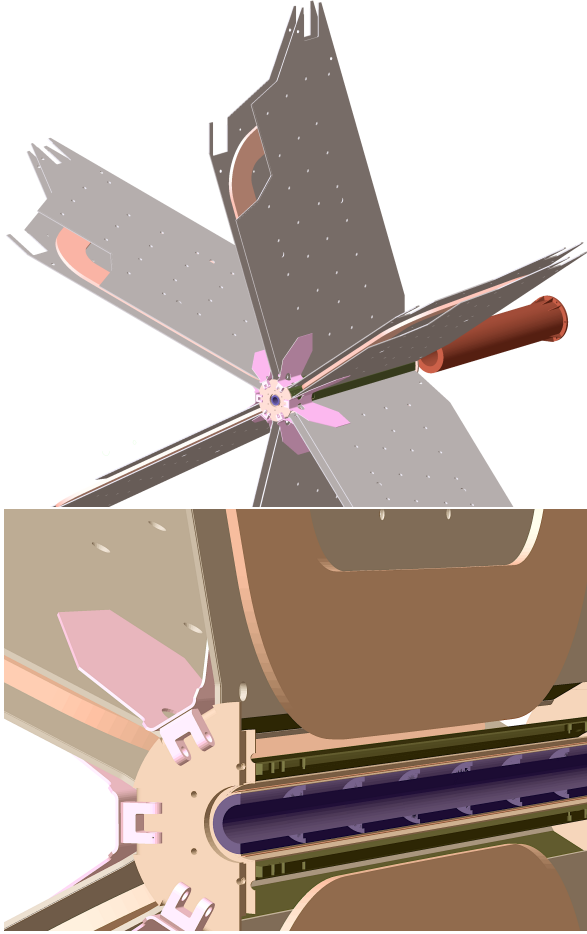

Figure 30: Top: the GEMC implementation of the torus hardware. The volumes are imported from the CAD engineering model. The stainless steel vacuum jacket embeds the Geant4 coil volumes. Bottom: a section view of the torus in the vicinity of the beamline. The warm and cold hubs are visible, along with the tungsten shielding in the innermost part of the hub. Beam is incident from the left.

24

The torus field in the sector midplane is perpendicular to the z-axis and is typically 2.058 T. Table 14 shows the field map ASCII data structure.

ϕ (deg)	T (m)	Z (m)	B_x	$B_y(T)$	B_z
0.0	190.0	338.0	0	0.451275	0
0.0	190.0	340.0	0	0.450136	0
0.0	190.0	342.0	0	0.448789	0
0.0	190.0	344.0	0	0.447235	0
0.0	190.0	346.0	0	0.445472	0
0.0	190.0	348.0	0	0.443502	0
0.0	190.0	350.0	0	0.441323	0
0.0	190.0	352.0	0	0.438935	0

Table 14: Torus ASCII field map values near mid-sector. T is the transverse coordinate $\sqrt{(x^2 + y^2)}$ and z is the longitudinal coordinate.

2.14. Beamline

The CLAS12 beamline geometry is entirely imported from the engineering CAD model. It is made up of several pieces, each discussed below. The positioning and composition of the beamline depend on the run configuration, which can be:

- FT-ON: Forward Tagger present and operational. The Møller shield starts at z=877 mm from the target center (see Fig. 32 top).

- FT-OFF: FT is present but not operational. The FT tracker is replaced by an additional shielding. The Møller shield starts at z=430 mm from the target center, and additional shielding is present to connect it to the FT (see Fig. 32 bottom).

2.14.1. Vacuum Pipe

The beamline is given by a stainless steel vacuum pipe that contains the electron beam. The pipe starts downstream of the target at z=80 cm and changes dimensions inside the torus and downstream of the torus as detailed in Table 15.

	Thickness (mm)	Inner Radius (mm)
Upstream	1.6	26.9
Inside	1.6	33.3
Downstream	3.2	60.3

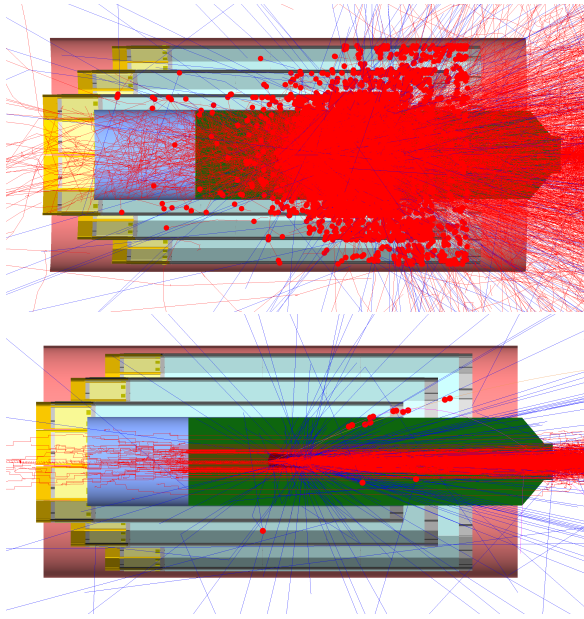Table 15: The vacuum beam pipe dimensions upstream, inside, and downstream of the torus.

Figure 31: An 11 GeV electron beam impinging on a 5-cm long liquid-hydrogen target. The SVT detector is shown. The figure shows one event at the full 10^{35} cm^{-2}s^{-1} luminosity, corresponding to 124,000 electrons in a 250 ns time window. Top: no solenoid field. A storm of Møller electrons saturates the SVT: each point is a recorded hit above the SVT threshold of 30 keV. Bottom: full solenoid field. The solenoid focuses the Møller electrons along the beamline, providing an effective electromagnetic shield for CLAS12.

25

Figure 33: The Møller shielding for the FT-ON configuration implemented in GEMC. On top a section of the overall overview of the cone, FT support, and torus mount. Various individual components are shown: the tungsten cone, the inner FT shield, and the structure of the torus mount.

2.14.2. Møller Shielding

The Møller shielding is composed of the following elements, shown in Fig. 33 for the FT-ON configuration and in Fig. 34 for the FT-OFF configuration.

- FT-ON and FT-OFF configurations:

  - a tungsten cone with increasing thickness;
  - a tungsten pipe and flange inside the FT;
  - a support system to mount the FT and the shielding onto the torus frame, composed by:
    * an inner stainless steel shield and flange
    * an outer tungsten shield
    * nine copper screws to adjust the alignment of the FT and shields upstream of the torus

- Additions for FT-OFF configuration:

  - a tungsten cone tip to extend the Møller shield cone;
  - lead cylinder in place of the FT tracker.

2.14.3. Torus and Downstream Shielding

Additional shielding is placed around the vacuum pipe through the torus magnet bore in the form of tungsten cylinders. Shielding downstream of the torus in the form of a connecting tungsten nose and a long lead cylinder enclosed by a stainless steel frame is also included [17].
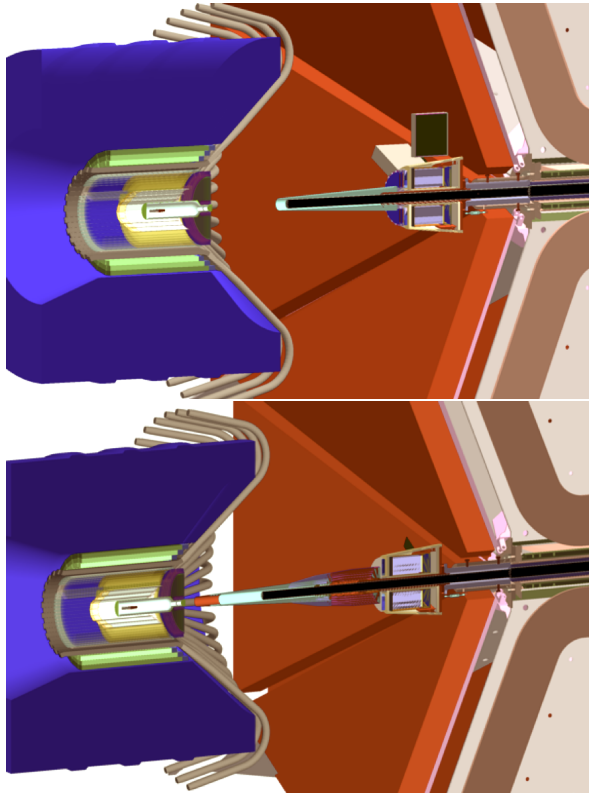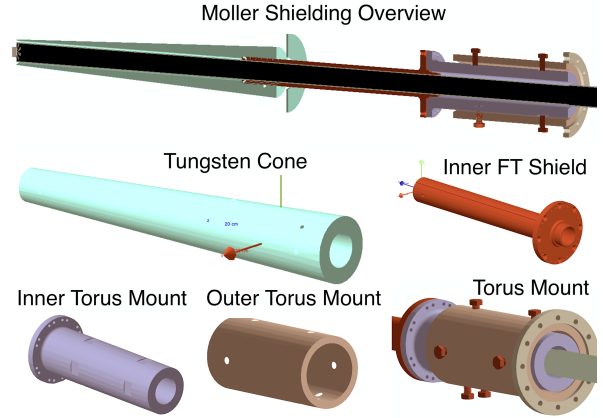

Figure 32: The two possible CLAS12 FT beamline configurations. Top: FT-ON. To clear its acceptance at forward angles (2.50°-4.50°), the Møller shield (cyan color) is attached to the FT tracker, starting at z=877 mm from the target. Bottom: FT-OFF; the FT is present but not operational. The FT tracker is replaced with a shield. The Møller cone is placed at z=430 mm from the target and additional shielding is added to minimize background in Region 1 DC.
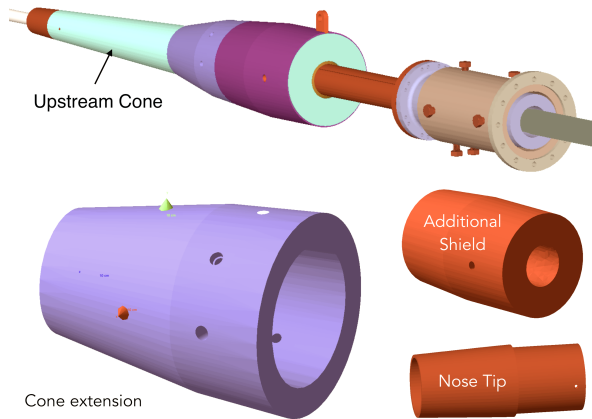
Figure 34: The Møller shielding for the FT-OFF configuration implemented in GEMC. Top: section of the overall overview of the cone, FT support, and torus mount. The cone tip extension and the additional shielding that replaces the FT tracker are also shown.

2.15. Summary of Detector Parameters

The CLAS12 detector parameters are summarized in Table 16. For most of the detectors the maximum step is set to a conservative 1 cm value. The actual step size in this case is decided by Geant4 using the cross sections tables, and will always be smaller than 1 cm. For the SVT, MM, and FT-Trk the maximum step is forced to be smaller than what Geant4 would choose, in order to correctly parameterize the electron avalanche paths that produce a signal in the strips. Wherever the FADC is used, the time window is set to the experimental electronics time window of 400 ns. The SVT, MM, and FT-Trk use a dedicated readout chip with shorter time windows. The Cherenkov detectors use 50-ns and the Drift Chambers use 500 ns.

3. Performance

The performance of the CLAS12 simulations is measured by comparing the predicted background rates from beam interactions in the target with the actual experimental rates. The benchmarks are also quantified for each detector geometry and digitization routine.

3.1. Comparison of Rates with Data

On December 17, 2017, the nominal luminosity of 1×10^{35} cm^{-2}s^{-1} (75 nA on a 5-cm long liquid-hydrogen target) was achieved in CLAS12 for the first time. The rates in each of the CLAS12 detectors were measured.

The drift chamber hit occupancy was compared for both the FT-ON and FT-OFF configurations. The integrated occupancy in Regions 1, 2, and 3 are summarized in Tables 17 and 18. The DC readout time windows of the experiment at the time were different than what was in the simulation, so the data has been scaled accordingly. The predicted rates agree quite well with the measured ones.

Similar agreements were found with the rates in the other CLAS12 detectors. In particular:

- FTOF: good agreement with data for the PMT currents [7];

- CTOF good agreement with data for the upstream PMT counter rates, while the downstream counter rates are about a factor of three lower in the simulation than they are in the data, probably due to the simulation not taking into account the Cherenkov light produced in the light guides [11];

- FT: good agreement with data for PMT currents and radiation doses [13].

3.2. Benchmarks

The GEMC event simulation rate has been measured for single and multiple tracks. The numbers reported here refer to averages over several 2017 laptops, desktops, and computing farm nodes, and refer to running GEMC in single-threaded mode. The full CLAS12 geometry has been used, with a Runge-Kutta field integration algorithm and linear interpolation for both the solenoid and the torus fields. Single meson tracks in the forward region are simulated with an event rate of about 10 Hz. The electron simulation takes about twice as long due to the shower simulations in the EC and PCAL calorimeters and Cherenkov photon production in both the HTCC and the LTCC, for an average rate of about 5 Hz.

A quantitative study of the event rate for 3 particles (2 in the Forward Detector, one in the Central Detector) details the time spent in each detector geometry, digitization, and magnetic field. The particles generated are:

- one 7 GeV electron between polar angles 15° and 25°;

- one 2 GeV photon between polar angles 15° and 25°;

- one 2 GeV proton at $\theta =90°$.

The results are shown in Table 19. The final rate for the 3 particles in the complete CLAS12 setup is 1.7 Hz. Simulations that include the complete beam-target interactions using the nominal luminosity of 10^{35} cm^{-2}s^{-1}

Detector	Geometry Source	Identifier	Digitized Output	Max Step	Time Window
SVT	JAVA service	sector, layer, strip	ADC	30 μmm	128 ns
MM	PERL API	sector, layer, strip	ADC	270 μmm	132 ns
CTOF	CAD	sector, layer, paddle	FADC, ADC, TDC	1 cm	400 ns
CND	PERL API	sector, layer, component	FADC, ADC, TDC	1 cm	400 ns
HTCC	PERL API	sector, ring, index	ADC	1 cm	50 ns
FT-Trk	PERL API	layer, component	ADC	300 μmm	132 ns
FT-Hodo	PERL API	sector, layer, component	FADC, ADC, TDC	1 cm	400 ns
FT-Cal	PERL API	component	FADC, ADC, TDC	1 cm	400 ns
DC	JAVA service	sector, layer, wire	TDC	1 mm	500 ns
LTCC	PERL API, CAD	sector, side, segment	ADC	1 cm	50 ns
RICH	PERL API, CAD	sector, pmt, pixel	TDCL, TDCL	1 cm	50 ns
FTOF	JAVA service	sector, layer, paddle	FADC, ADC, TDC	1 cm	400 ns
ECAL	JAVA service	sector, layer, strip	FADC, ADC, TDC	1 cm	400 ns

Table 16: Summary of the detector parameters. For the RICH detector, two TDCs are quoted that refer to the leading and trailing edge times of the signal.

Region	Data (re-scaled)	GEMC
1	2.8%	2.7%
2	0.6%	0.8%
3	1.5%	1.2%

Table 17: Drift chamber hit occupancy comparison between simulation and data for the FT-ON configuration at full luminosity.

Region	Data (re-scaled)	GEMC
1	1.7%	1.1%
2	0.3%	0.4%
3	0.9%	0.7%

Table 18: Drift chambers hit occupancy comparison between simulation and data for the FT-OFF configuration at full luminosity.

are made using 124,000 electrons per event. In this case the time to complete one event varies between one and two minutes depending on the CPU type and available memory.

4. Distribution and Documentation

The GEMC framework is documented on the GEMC website [14]. This includes the latest news and releases, examples, procedure details, and documentation for all of the available options. The software is distributed in two ways: with Docker [35] or by downloading the source from the public git repository.

A Docker container with the necessary libraries to run GEMC and the reconstruction software is created in the
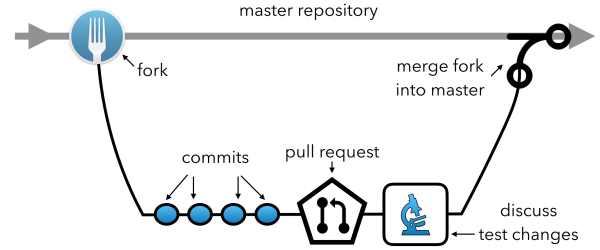

Figure 35: Typical workflow of contribution to the code. First, the main repository is forked and worked on. Then, during the fork code developments, comments can be made on the various commits. Lastly, when the users make the pull request, the changes are validated and then merged to the master repository (or sent back with comments if there were problems).

Jefferson Lab hub repository. The container is tagged, and every tag contains a set version of these libraries:

- PYTHIA-based event generators for various physics channels relevant to the CLAS12 analyses;

- GEMC with the CLAS12 geometry;

- the JAVA reconstruction software [18].

The code git repository is `https://github.com/gemc/source`, which is a public repository. The development contribution mechanism is illustrated in Fig. 35: collaborators fork the repository and make pull requests that are validated by the code author. GEMC is released on a semi-annual cycle.

The list of software packages included in the GEMC framework is:

System	event rate (ms)	% of total
Target	1.2	0.20
SVT	0.9	0.16
CTOF	0.4	0.06
CND	0.2	0.04
Solenoid	33.9	5.77
MM	26.1	4.44
HTCC	20.5	3.49
Torus	45.1	7.66
FT	10.5	1.78
DC	48.3	8.21
RICH	23.6	4.01
LTCC	27.6	4.69
FTOF	11.3	1.02
PCAL	186.2	31.67
EC	152.4	25.91
CLAS12	588.1	100

Table 19: GEMC simulation benchmarks in each CLAS12 detector and magnet. The time spent (by swimming and digitization) within each system by 3 particles (2 in the Forward Detector, one in the Central Detector) is tabulated. The calorimeters are responsible for more than half the computing time, due to shower simulations. Swimming in the magnetic fields accounts for about 13.5% of the total CPU time. The overall rate for the full CLAS12 detector is 1.7 Hz.

- CLHEP: Class Library for High Energy Physics [36];

- XERCESC: validating XML parser [37];

- Geant4: the libraries to simulate the passage of particles through matter [15];

- QT: a C++ graphic library [38];

- EVIO: the CLAS12 data format [26];

- CCDB: the calibration database based on MYSQL [25].

The main documentation is on the GEMC website [14]. It includes examples of how to create and run a custom geometry and use various features like event generators, geometry factories, hit definitions, output, etc.

The CLAS12 development of both hit process routines and geometry is kept on the CLAS12 tags portal [19], which also contains documentation on how to run with configurations corresponding to the various experiments, how to change the beamline configuration, and how to switch between code and geometry releases.

5. Conclusions

In this paper the GEMC Geant4 implementation of the CLAS12 detector is presented. Thanks to the flexibility of C++ and Geant4, and the power of object-oriented programming, a detailed Geant4 simulation of the CLAS12 detectors was developed in which the geometry, digitization, and simulation parameters were decoupled from the code. This allowed the geometry to be implemented through several sources: native Geant4 volumes, imports from CAD engineering models, and CLAS12 JAVA geometry services. Realistic detector responses that make use of the data calibration constants to provide output distributions comparable to the data are included using plugin-like algorithms. The data acquisition response is reproduced by electronic time window algorithms.

The framework has been shown to perform very well when comparing simulation rates to data and it was an essential component to optimize the design of the CLAS12 detectors, their associated calibration procedures, and their ultimate performance. GEMC is an essential tool for improving the significance and accuracy of the physics analyses and for realizing the science goals of the CLAS Collaboration.

6. Acknowledgments

7. References

[1] V. D. Burkert, et al., The CLAS12 Spectrometer at Jefferson Laboratory, to be published in Nucl. Inst. and Meth. A, (2020) (see this issue).

[2] R. Fair, et al., The CLAS12 Superconducting Magnets, to be published in Nucl. Inst. and Meth. A, (2020) (see this issue).

[3] M. D. Mestayer, The CLAS12 Drift Chamber System, to be published in Nucl. Inst. and Meth. A, (2020) (see this issue).

[4] M. Ungaro, et al., The CLAS12 Low Threshold Cherenkov Counter, to be published in Nucl. Inst. and Meth. A, (2020) (see this issue).

[5] Y. G. Sharabian, et al., The CLAS12 High Threshold Cherenkov Counter, to be published in Nucl. Inst. and Meth. A, (2020) (see this issue).

[6] M. Contalbrigo, et al., The CLAS12 Ring Imaging Cherenkov Detector, to be published in Nucl. Inst. and Meth. A, (2020) (see this issue).

[7] D. S. Carman, et al., The CLAS12 Forward Time-of-Flight System, to be published in Nucl. Inst. and Meth. A, (2020) (see this issue).

[8] G. Asryan, et al., The CLAS12 Pre-Shower Calorimeter, to be published in Nucl. Inst. and Meth. A, (2020) (see this issue).

[9] M. A. Antonioli, et al., The CLAS12 Silicon Vertex Tracker, to be published in Nucl. Inst. and Meth. A, (2020) (see this issue).

[10] A. Acker, et al., The CLAS12 Micromegas Vertex Tracker, to be published in Nucl. Inst. and Meth. A, (2020) (see this issue).

[11] D. S. Carman, et al., The CLAS12 Central Time-of-Flight System, to be published in Nucl. Inst. and Meth. A, (2020) (see this issue).

[12] P. Chatagnon, et al., The CLAS12 Central Neutron Detector, to be published in Nucl. Inst. and Meth. A, (2020) (see this issue).

[13] A. Acker, et al., The CLAS12 Forward Tagger, to be published in Nucl. Inst. and Meth. A, (2020) (see this issue).

[14] M. Ungaro, GEMC: A Geant4 simulation framework.
URL https://gemc.jlab.org

[15] S. Agostinelli, et al., Geant4a simulation toolkit, Nuclear Instruments and Methods in Physics Research 506 (3) (2003) 250–303. doi:10.1016/S0168-9002(03)01368-8.

[16] M. Amarian, et al., The CLAS forward electromagnetic calorimeter, Nucl. Instrum. Meth. A460 (2001) 239–265. doi:10.1016/S0168-9002(00)00996-7.

[17] N. Baltzell, et al., The CLAS12 Beamline and its Performance, to be published in Nucl. Inst. and Meth. A, (2020) (see this issue).

[18] V. Ziegler, et al., The CLAS12 Software Framework and Event Reconstruction, to be published in Nucl. Inst. and Meth. A, (2020) (see this issue).

[19] M. Ungaro, The CLAS12 Simulation Software and Geometry repository.
URL https://clasweb.jlab.org/clas12/clas12SoftwarePage/html/index.html

[20] Wikipedia, The STEP file format.
URL https://en.wikipedia.org/wiki/ISO_10303-21

[21] The FreeCAD Team, FreeCad: a 3D parametric modeler.
URL https://www.freecadweb.org

[22] Wikipedia, RungeKutta methods.
URL https://en.wikipedia.org/wiki/RungeKutta_methods

[23] S. Boyarinov, et al., The CLAS12 Data Acquisition System, to be published in Nucl. Inst. and Meth. A, (2020) (see this issue).

[24] B. Raydo, et al., The CLAS12 Trigger System, to be published in Nucl. Inst. and Meth. A, (2020) (see this issue).

[25] The Calibration Constant Database wikipage.
URL https://github.com/JeffersonLab/ccdb/wiki

[26] Jefferson Lab Data Acquisition, The EVIO data format.
URL https://coda.jlab.org/drupal/content/event-io-evio

[27] I. Antcheva, et al., ROOT: A C++ framework for petabyte data storage, statistical analysis and visualization, Comput. Phys. Commun. 182 (2011) 1384–1385. doi:10.1016/j.cpc.2011.02.008.

[28] M. Ungaro, Corrections to CLAS12 Target Design, CLAS12 Technical Note 2017-013.
URL https://misportal.jlab.org/mis/physics/clas12/viewFile.cfm/2017-013.pdf?documentId=48

[29] V. D. Burkert, S. Stepanyan, J. A. Tan, M. Ungaro, Beam Position Study on a 3.5 mm Shifted Target Cell, CLAS12 Technical Note 2017-18.
URL https://misportal.jlab.org/mis/physics/clas12/viewFile.cfm/2017-018.pdf?documentId=54

[30] V. D. Burkert, Y. Gotra, M. Ungaro, Study of Tungsten Shielding Around the CLAS12 Target, CLAS12 Technical Note 2018-005.
URL https://misportal.jlab.org/mis/physics/clas12/viewFile.cfm/2018-005.pdf?documentId=59

[31] R. D. Vita, M. Ungaro, Importing CLAS12 CAD Models of Target and Beamline in the GEMC Simulation, CLAS12 Technical Note 2017-17.
URL https://misportal.jlab.org/mis/physics/clas12/viewFile.cfm/2017-017.pdf?documentId=53

[32] R. D. Vita, L. Elouadrhiri, A. Kim, R. Miller, S. Stepanyan, J. A. Tan., M. Ungaro, C. Wiggins, M. Zarecky, Corrections to CLAS12 Vacuum Beamline, CLAS12 Technical Note 2017-012.
URL https://misportal.jlab.org/mis/physics/clas12/viewFile.cfm/2017-012.pdf?documentId=47

[33] R. D. Vita, D. S. Carman, C. Smith, S. Stepanyan, M. Ungaro, Study of the Electromagnetic Background Rates in CLAS12, CLAS12 Technical Note 2017-16.
URL https://misportal.jlab.org/mis/physics/clas12/viewFile.cfm/2017-016.pdf?documentId=52

[34] P. K. Ghoshal, J. M. Beck, R. J. Fair, D. H. Kashy, M. D. Mestayer, J. Meyers, J. Newton, R. Rajput-Ghoshal, K. Tremblay, C. L. Wiggins, Magnetic Field Mapping of the CLAS12 Torus: A Comparative Study Between the Engineering Model and Measurements at JLab, IEEE Trans. Appl. Supercond. 29 (4) (2018) 4000310. doi:10.1109/TASC.2018.2884968.

[35] The Jefferson Lab Docker Hub.
URL https://cloud.docker.com/u/jeffersonlab

[36] The CLHEP project, CLHEP - A Class Library for High Energy Physics.
URL http://proj-clhep.web.cern.ch/proj-clhep

[37] The Apache XML project, The Xerces-C++ XML Parser.
URL https://xerces.apache.org/xerces-c

[38] The QT Company, QT: a cross-platform SDK.
URL https://www.qt.io